

Typical-Medium Theory of Mott-Anderson Localization

V. Dobrosavljević

*Department of Physics and National High Magnetic Field Laboratory
Florida State University, Tallahassee, Florida 32310*

The Mott and the Anderson routes to localization have long been recognized as the two basic processes that can drive the metal-insulator transition (MIT). Theories separately describing each of these mechanisms were discussed long ago, but an accepted approach that can include both has remained elusive. The lack of any obvious static symmetry distinguishing the metal from the insulator poses another fundamental problem, since an appropriate *static* order parameter cannot be easily found. More recent work, however, has revisited the original arguments of Anderson and Mott, which stressed that the key difference between the metal and the insulator lies in the dynamics of the electron. This physical picture has suggested that the “typical” (geometrically averaged) escape rate $\tau_{typ}^{-1} = \exp(\ln \tau_{esc}^{-1})$ from a given lattice site should be regarded as the proper *dynamical order parameter* for the MIT, one that can naturally describe both the Anderson and the Mott mechanism for localization. This article provides an overview of the recent results obtained from the corresponding *Typical-Medium Theory*, which provided new insight into the two-fluid character of the Mott-Anderson transition.

I. FROM METAL TO INSULATOR: A NEW PERSPECTIVE

Metal or insulator - and why? To answer this simple question has been the goal and the driving force for much of the physical science as we know it today. Going back to Newton’s not-so-successful exercises in Alchemy, the scientist had tried to understand what controls the flow of electricity in metals and what prevents it in insulators [1]. To understand it and to control it - achieving this could prove more useful and lucrative than converting lead into gold. Indeed, the last few decades have witnessed some most amazing and unexpected advances in material science and technology. And this ability - its intellectual underpinning - is what was indispensable in designing and fabricating the iPhone, the X-Box, and the MRI diagnostic tool. Today’s kids have grown up in a different world than had their parents - all because we have learned a few basic ideas and principles of electron dynamics.

In almost every instance, these advances are based on materials that find themselves somewhere between metals and insulators. Material properties are easy to tune in this regime, where several possible ground states compete [5]. Here most physical quantities display unusual behavior [6], and prove difficult to interpret using conventional ideas and approaches. Over the last few decades, scores of theoretical scenarios and physical pictures have been proposed, most of which will undoubtedly end up in back drawers of history. Last couple of years, however, have seen a veritable avalanche of new experimental results, which provide compelling clues as to what the theorists should not overlook: the significant effects of spatial inhomogeneities in the midst of strongly correlated phases.

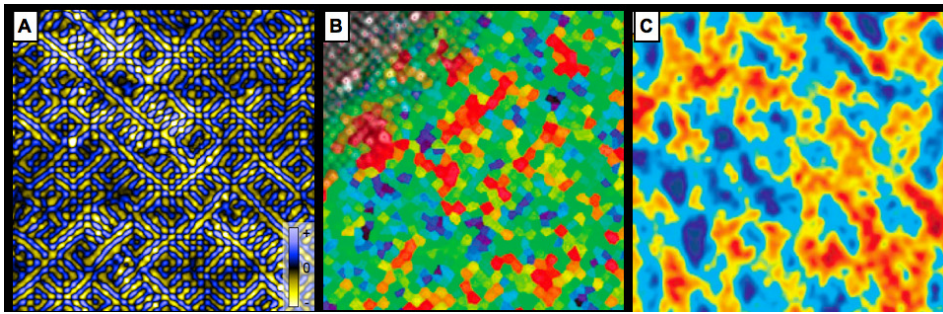


Figure 1: Spectacular advances in scanning tunneling microscopy (STM) have revealed that many “bad metals” or barely-doped insulators are surprisingly inhomogeneous on the nano-scale. Understanding and controlling these materials will not be possible without coming to grips with the origin, the stability, and the statistics of such mesoscopic granularity. (A) “Tunneling asymmetry” imaging [2] provides evidence for the emergence of a low temperature “electronic cluster glass” within the superconducting phase of $Ca_{1.88}Na_{0.12}CuO_2Cl_2$; (B) Fourier-transform STM [3] reveals nano-scale Fermi surface variations in $Bi_2Sr_2CuO_{6-x}$; (C) Differential conductance maps [4] showing spatial variations of the local pseudogaps in the normal phase ($T \gg T_c$) of $Bi_2Sr_2CaCu_2O_{8+\delta}$.

To understand many, if not most exotic new materials, one has to tackle the difficult problem of understanding the metal-insulator quantum phase transition, as driven by the combined effects of strong electronic correlations and disorder. Traditional approaches to the problem, which emerged in the early 1980s, have focused on examining the perturbative effects of disorder within the Fermi liquid framework. Despite their mathematical elegance, these theories, unfortunately, prove ill-suited to describe several key physical processes, such as tendency to local magnetic moment formation and the approach to the Mott insulating state. In addition, such weak-coupling theories cannot easily describe strongly inhomogeneous phases, with behavior often dominated by broad distributions and rare disorder configurations.

This new insight, which is largely driven by experimental advances, seems to suggest that an alternative theoretical picture may provide a better starting point. In this article we describe recent advances based on a new theoretical method, which offers a complementary perspective to the conventional weak-coupling theories. By revisiting the original ideas of Anderson and Mott, it examines the *typical escape rate* from a given site as the fundamental *dynamical order parameter* to distinguish between a metal and an insulator. This article describes the corresponding *Typical-Medium Theory (TMT)* and discusses some of its recent results and potential applications. We first discuss, in some detail, several experimental and theoretical clues suggesting that a new theoretical paradigm is needed. The formulation of TMT for Anderson localization of noninteracting electrons is then discussed, with emphasis on available analytical results. Finally, we review recent progress in applying TMT to the Mott-Anderson transition for disordered Hubbard models, and discuss resulting the two-fluid behavior at the critical point.

II. THEORETICAL CHALLENGES: BEYOND CINDERELLA'S SLIPPER?

The existence of a sharp metal-insulator transition at $T = 0$ has been appreciated for many years [1]. Experiments on many systems indeed have demonstrated that a well defined critical carrier concentration can easily be identified. On the theoretical side, ambiguities on how to describe or even think of the metal-insulator transition have made it difficult to directly address the nature of the critical region. In practice, one often employs the theoretical tools that are available, even if possibly inappropriate. Even worse, one often focuses on those systems and phenomena that fit an available theoretical mold, ignoring and brushing aside precisely those features that seem difficult to understand. This “Cinderella’s slipper” approach is exactly what one should not do; unfortunately it happens all too often. A cure is, of course, given by soberly confronting the experimental reality: what seems paradoxical at first sight often proves to be the first clue to the solution.

A. Traditional approaches to disordered interacting electrons

Most studies carried out over the last thirty years have focused on the limit of weak disorder [7], where considerable progress has been achieved. Here, for non-interacting electrons the conductance was found to acquire singular (diverging) corrections in one and two dimensions, an effect known as “weak localization” [7, 8]. According to these predictions, for $d \leq 2$ the conductivity would monotonically decrease as the temperature is lowered, and would ultimately lead to an insulating state at $T = 0$. Interestingly, similar behavior was known in Heisenberg magnets [9–11], where it resulted from $d = 2$ being the *lower critical dimension* for the problem. This analogy with conventional critical phenomena was first emphasized by the “gang of four” [8], as well as Wegner [9, 10], who proposed an approach to the metal-insulator transition based on expanding around two dimensions. For this purpose, an effective low energy description was constructed [9, 10, 12], which selects those processes that give the leading corrections at weak disorder in and near two dimensions. This “non-linear sigma model” formulation [9, 10, 12] was subsequently generalized to interacting electrons by Finkel’shtein [13], and studied using renormalization group methods in $2 + \varepsilon$ dimensions [13–15]. In recent years, the non-linear sigma model of disordered interacting electrons has been extensively studied by several authors [16, 17].

While the sigma model approach presented considerable formal complexity, its physical content proved - in fact - to be remarkably simple. As emphasized by Castellani, Kotliar and Lee [18], one can think of the sigma model of disordered interacting electrons as a low energy *Fermi liquid* description of the system. Here, the low energy excitations are viewed as a gas of diluted quasi-particles that, at least for weak disorder, can be described by a small number of Fermi liquid parameters such as the diffusion constant, the effective mass, and the interaction amplitudes. In this approach, one investigates the evolution of these Fermi liquid parameters as weak disorder is introduced. The metal-insulator transition is then identified by the *instability* of this Fermi liquid description, which in $d = 2 + \varepsilon$ dimensions happens at weak disorder, where controlled *perturbative* calculations can be carried out.

Remarkably, by focusing on such a stability analysis of the metallic state, one can develop a theory for the transition which does not require an *order parameter* description, in contrast to the standard approaches to critical phenomena [11]. This is a crucial advantage of the sigma model approach, precisely because of the ambiguities in defining an appropriate order parameter. We should stress, however, that by construction, the sigma model focuses on those physical processes that dominate the perturbative, weak disorder regime. In real systems, the metal-insulator transition is found at strong disorder, where a completely different set of processes could be at play.

B. Anderson’s legacy: strong disorder fluctuations

From a more general point of view, one may wonder how pronounced are the effects of disorder on quantum phase transitions. Impurities and defects are present in every sample, but their full impact has long remained ill-understood. In early work, Griffiths discovered [19, 20] that rare events due to certain types of disorder can produce nonanalytic corrections in thermodynamic response. Still, for classical models and thermal phase transitions he considered, these effects are so weak to remain unobservably small [21]. The critical behavior then remains essentially unmodified.

More recent efforts turned to quantum ($T = 0$) phase transitions [22], where the rare disorder configurations prove much more important. In some systems they give rise to “Quantum Griffiths Phases” (QGP) [6, 23], associated with the “Infinite Randomness Fixed Point” (IRFP) phenomenology [24]. Here, disorder effects produce singular thermodynamic response not only at the critical point, but over *an entire region* in its vicinity. In other cases, related disorder effects are predicted [25, 26] to result in “rounding” of the critical point, or to produce intermediate “cluster glass” phases [27, 28] masking the critical point. Physically, QGP-IRFP behavior means [6, 23] that very close to the critical point, the system looks increasingly inhomogeneous even in static response.

But how robust and generic may such pronounced sensitivity to disorder be in real systems? Does it apply only to (magnetic and/or charge) ordering transitions, or is it relevant also for the metal-insulator transitions (MITs)? A conclusive answer to these questions begs the ability to locally visualise the system on the nano-scale. Remarkably, very recent STM images provide striking evidence of dramatic spatial inhomogeneities in surprisingly many systems. While much more careful experimental and theoretical work is called for, these new insights make it abundantly clear that strong disorder effects - as first emphasized by early seminal work of Anderson [32] - simply cannot be disregarded.

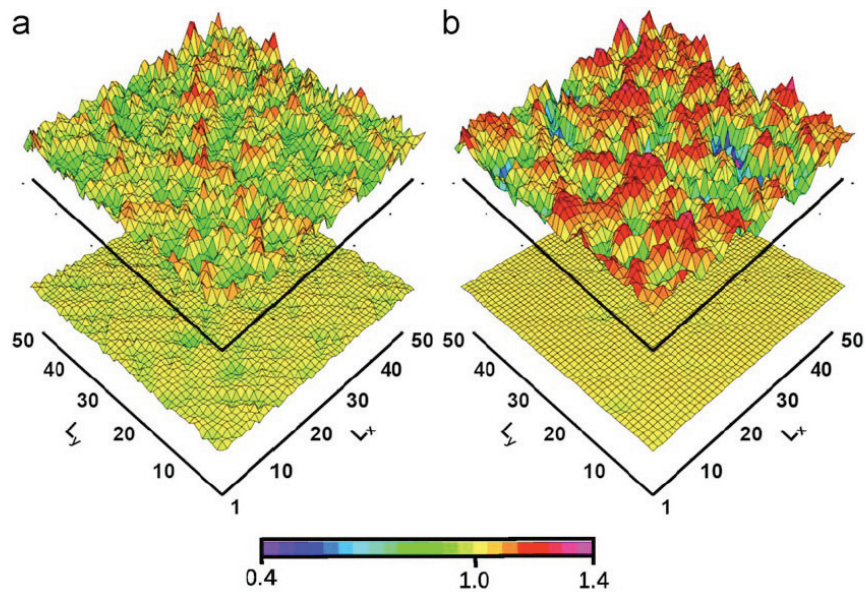


Figure 2: Theory predictions [29] for an “Electronic Griffiths Phase” [30] in a moderately disordered normal metal near a Mott metal-insulator transition. Local density of states (LDOS) spectra look dramatically “smoother” near the Fermi energy (bottom) than away from it (top). This contrast is more pronounced close to the Mott transition (right), than outside the critical region (left). Very similar behavior was recently observed by STM imaging of the superconducting phase of doped cuprates [2], but our results strongly suggest that such energy-resolved “disorder healing” [29–31] is a much more general property of Mott systems.

C. The curse of Mottness: the not-so-Fermi liquids

One more issue poses a major theoretical challenge. According to Landau's Fermi liquid theory, any low temperature metal behaves in a way very similar to a gas of weakly interacting fermions. In strongly correlated systems, closer to the Mott insulating state, this behavior is typically observed only below a modest crossover temperature $T^* \ll T_F$. Adding disorder typically reduces T^* even further, and much of the experimentally relevant temperature range simply does not conform to Landau's predictions. Theoretically, this situation poses a serious problem, since the excitations in this regime no longer assume the character of diluted quasiparticles. Here perturbative corrections to Fermi liquid theory simply do not work [6], and a conceptually new approach is needed.

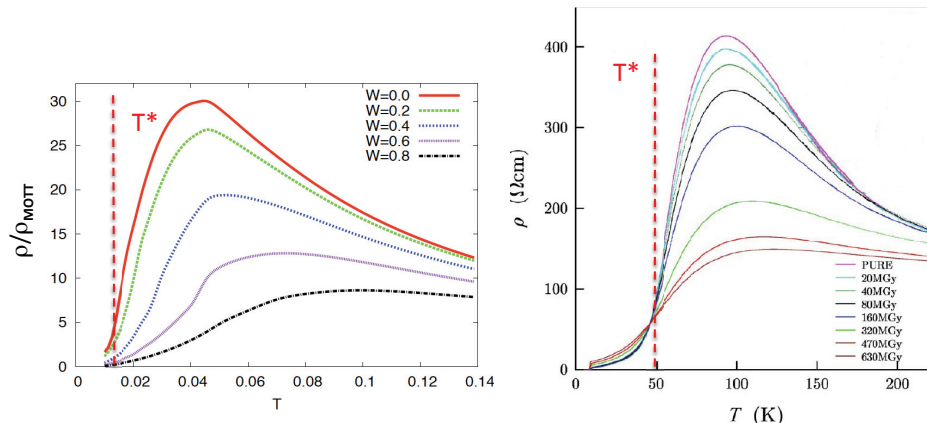


Figure 3: Finite temperature metal-insulator crossover in transport close to a disordered Mott transition. Very high values of resistivity, strongly exceeding the “Mott limit” [1, 33] are observed above the crossover temperature T^* . Remarkably, increasing disorder W reduces the resistivity maximum, rendering the system effectively more metallic. This behavior, which is clearly seen in our DMFT modelling [34] (left panel), has very recently been also observed in experiments [35] on organic charge-transfer salts (right panel), where disorder is systematically introduced by X-ray irradiation.

A new theoretical paradigm, which works best precisely in the incoherent metallic regime, has been provided by the recently developed *Dynamical Mean-Field Theory* (DMFT) methods [36]. Unfortunately, in its original formulation, which is strictly exact in the limit of infinite dimensions, DMFT is not able to capture Anderson localization effects. Over the last twelve years, this nonperturbative approach has been further extended [6, 37–44] to incorporate the interplay between the two fundamental mechanisms for electron localization: the Mott (interaction-driven) [1] and the Anderson (disorder-driven) [32, 45] route to arrest the electronic motion. In addition, the DMFT formulation can be very naturally extended to also describe strongly inhomogeneous and glassy phases of electrons [46–55], and even capture some aspects of the Quantum Griffiths Phase physics found at strong disorder [6, 27, 28, 39, 40, 44, 56–63]. In the following, we first discuss the DMFT method as a general order-parameter theory for the metal-insulator transition, and then explain how it needs to be modified to capture Anderson localization effects.

III. ORDER-PARAMETER APPROACH TO INTERACTION-LOCALISATION

A. Need for an order-parameter theory: experimental clues

In conventional critical phenomena, simple mean-field approaches such as the Bragg-Williams theory of magnetism, or the Van der Waals theory for liquids and gases work remarkably well - everywhere except in a very narrow critical region. Here, effects of long wavelength fluctuations emerge that modify the critical behavior, and its description requires more sophisticated theoretical tools, based on renormalization group (RG) methods. A basic question then emerges when looking at experiments: is a given phenomenon a manifestation of some underlying mean-field (local) physics, or is it dominated by long-distance correlations, thus requiring an RG description? For conventional criticality the answer is well known, but how about metal-insulator transitions? Here the experimental evidence is much more limited, but we would like to emphasize a few well-documented examples which stand out.

1. Doped semiconductors

Doped semiconductors such as Si:P [64] are the most carefully studied examples of the MIT critical behavior. Here the density-dependent conductivity extrapolated to $T = 0$ shows sharp critical behavior [65] of the form $\sigma \sim (n - n_c)^\mu$, where the critical exponent $\mu \approx 1/2$ for uncompensated samples (half-filled impurity band), while dramatically different $\mu \approx 1$ is found for heavily compensated samples of Si:P,B, or in presence of strong magnetic fields. Most remarkably, the dramatic differences between these cases is seen over an extremely broad concentration range, roughly up to several times the critical density. Such robust behavior, together with simple apparent values for the critical exponents, seems reminiscent of standard mean-field behavior in ordinary criticality.

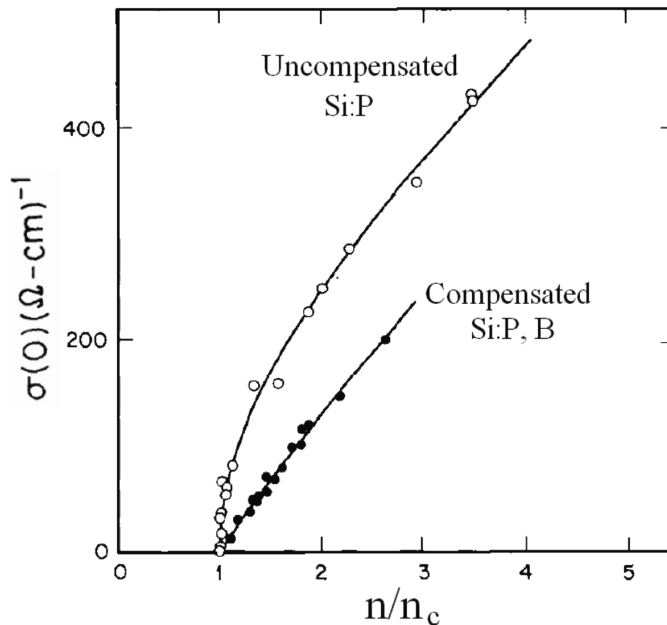


Figure 4: Critical behavior of the conductivity for uncompensated Si:P and compensated Si:P,B [65]. The conductivity exponent $\mu \approx 1/2$ in absence of compensation, while $\mu \approx 1$ in its presence. Clearly distinct behavior is observed in a surprisingly broad range of densities, suggesting mean-field scaling. Since compensation essentially corresponds to carrier doping away from a half-filled impurity band [64], it has been suggested [7] that the difference between the two cases may reflect the role of strong correlations.

2. 2D-MIT

Signatures of a remarkably sharp metal-insulator transition has also been observed [66–68] in several examples of two-dimensional electron gases (2DEG) such as silicon MOSFETs. While some controversy regarding the nature or even the driving force for this transition remains a subject of intense debate, several experimental features seem robust properties common to most studied samples and materials. In particular, various experimental groups have demonstrated [66, 67] striking scaling of the resistivity curves in the critical region, which seems to display [69] remarkable mirror symmetry (“duality”) [70] over a surprisingly broad interval of parameters. In addition, the characteristic behavior extends to remarkably high temperatures, which are typically comparable the Fermi temperature [68]. One generally does not expect a Fermi liquid picture of diluted quasiparticles to apply at such “high energies”, or any correlation length associated with quantum criticality to remain long.

These experiments taken together provide strong hints that an appropriate mean-field description is what is needed. It should provide the equivalent of the Van der Waals equation of state, for disordered interacting electrons. Such a theory has long been elusive, primarily due to a lack of a simple order-parameter formulation for this problem. Very recently, an alternative approach to the problem of disordered interacting electrons has been formulated, based on dynamical mean-field (DMFT) methods [36]. This formulation is largely complementary to the scaling approach, and has already resulting in several striking predictions. In the following, we briefly describe this method, and summarize the main results that have been obtained so far.

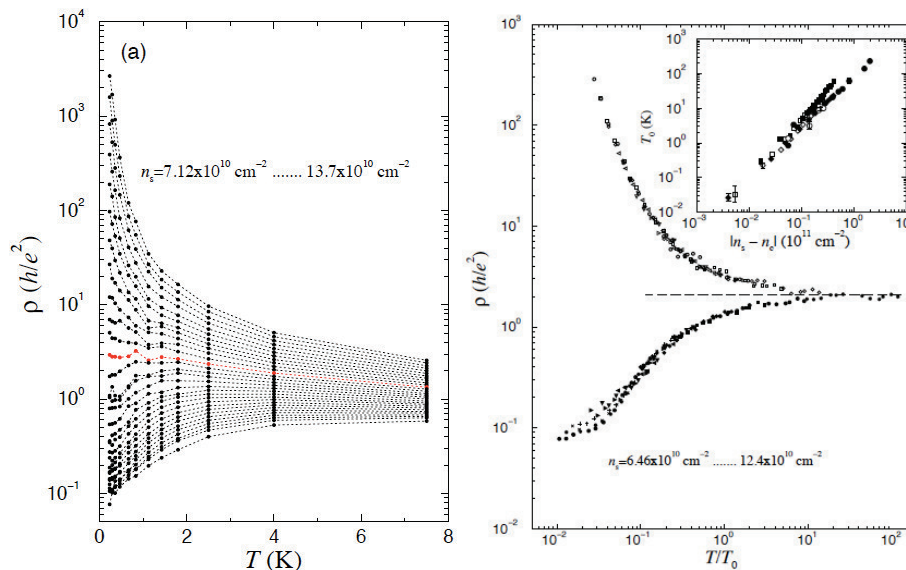


Figure 5: The resistivity curves (left panel) for a two-dimensional electron system in silicon [66] show a dramatic metal-insulator crossover as the density is reduced below $n_c \sim 10^{11} \text{cm}^{-2}$. Note that the system has “made up its mind” whether to be a metal or an insulator even at surprisingly high temperatures $T \sim T_F \approx 10 \text{K}$. The right panel displays the scaling behavior which seems to hold over a comparable temperature range. The remarkable “mirror symmetry” [69] of the scaling curves seems to hold over more than an order of magnitude for the resistivity ratio. This surprising behavior has been interpreted [70] as evidence that the transition region is dominated by strong coupling effects characterizing the insulating phase.

B. The DMFT physical picture

The main idea of the DMFT approach is in principle very close to the original Bragg-Williams (BW) mean-field theories of magnetism [71]. It focuses on a single lattice site, but replaces [36] its environment by a self-consistently determined “effective medium”, as shown in Fig. 1.3.

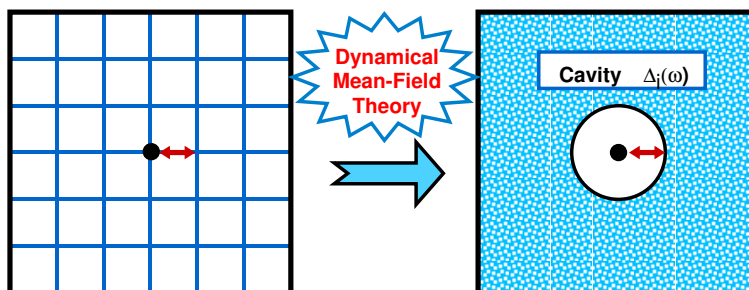


Figure 6: In dynamical mean-field theory, the environment of a given site is represented by an effective medium, represented by its “cavity spectral function” $\Delta_i(\omega)$. In a *disordered* system, $\Delta_i(\omega)$ for different sites can be very different, reflecting Anderson localization effects.

In contrast to the BW theory, the environment cannot be represented by a static external field, but instead must contain the information about the dynamics of an electron moving in or out of the given site. Such a description can be made precise by formally integrating out [36] all the degrees of freedom on other lattice sites. In presence of electron-electron interactions, the resulting local effective action has an arbitrarily complicated form. Within DMFT, the situation simplifies, and all the information about the environment is contained in the local single particle spectral function $\Delta_i(\omega)$. The calculation then reduces to solving an appropriate quantum impurity problem supplemented by an additional self-consistency condition that determines this “cavity function” $\Delta_i(\omega)$.

The precise form of the DMFT equations depends on the particular model of interacting electrons and/or the form of disorder, but most applications [36] to this date have focused on Hubbard and Anderson lattice models. The approach has been very successful in examining the vicinity of the Mott transition in clean systems, in which it has met spectacular successes in elucidating various properties of several transition metal oxides [40], heavy fermion systems, and even Kondo insulators [72].

C. DMFT as an order-parameter theory for the MIT

The central quantity in the DMFT approach is the local “cavity” spectral function $\Delta_i(\omega)$. From the physical point of view, this object essentially represents the *available electronic states* to which an electron can “jump” on its way out of a given lattice site. As such, it provides a natural order parameter description for the MIT. Of course, its form can be substantially modified by either the electron-electron interactions or disorder, reflecting the corresponding modifications of the electron dynamics. According to Fermi’s golden rule, the transition rate to a neighboring site is proportional to the density of final states - leading to insulating behavior whenever $\Delta_i(\omega)$ has a gap at the Fermi energy. In the case of a Mott transition in the absence of disorder, such a gap is a direct consequence of the strong on-site Coulomb repulsion, and is the same for every lattice site.

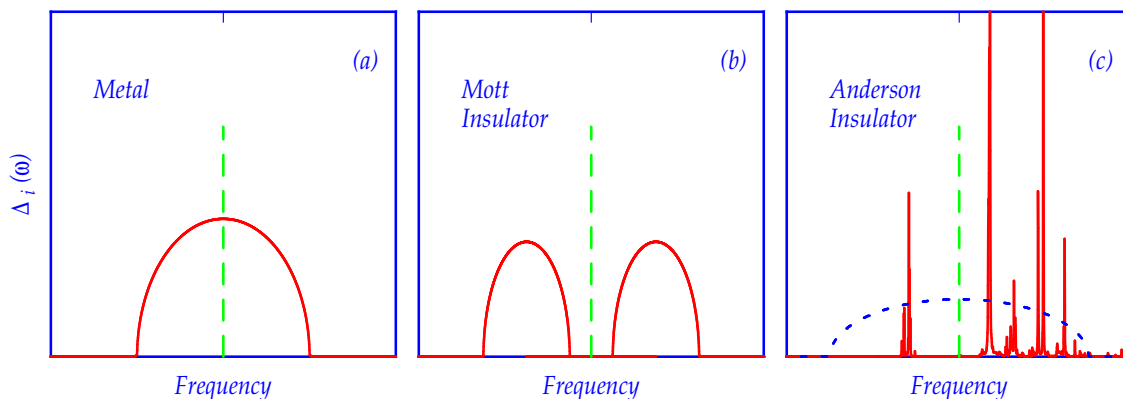


Figure 7: The local cavity spectral function $\Delta_i(\omega)$ as the order parameter for the MIT. In a metal (a) there are available electronic states near the Fermi level (dashed line) to which an electron from a given site can delocalize. Both for a Mott insulator (b) and the Anderson insulator (c) the Fermi level is in the gap, and the electron cannot leave the site. Note that the *averaged* spectral function (dotted line in (c)) has no gap for the Anderson insulator, and thus cannot serve as an order parameter.

The situation is more subtle in the case of disorder-induced localization, as first noted in the pioneering work of Anderson [32]. Here, the *average* value of $\Delta_i(\omega)$ has no gap and thus cannot serve as an order parameter. However, as Anderson noted a long time ago, “...no real atom is an average atom...” [45]. Indeed, in an Anderson insulator, the environment “seen” by an electron on a given site can be very different from its average value. In this case, the *typical* “cavity” spectral function $\Delta_i(\omega)$ consists of several delta-function (sharp) peaks, reflecting the existence of localized (bound) electronic states, as shown in Fig. 1.4(c). Thus a *typical* site is embedded in an environment that has a *gap* at the Fermi energy - resulting in insulating behavior. We emphasize that the location and width of these gaps strongly vary from site to site. These strong fluctuations of the local spectral functions persist on the metallic side of the transition, where the typical spectral density $\Delta_{typ} = \exp \langle \ln(\Delta_i) \rangle$ can be much smaller than its average value. Clearly, a full *distribution function* is needed to characterize the system. The situation is similar as in other disordered systems, such as spin glasses [73]. Instead of simple averages, here the entire distribution function plays a role of an order parameter, and undergoes a qualitative change at the phase transition.

The DMFT formulation thus naturally introduces self-consistently defined order parameters that can be utilized to characterize the qualitative differences between various phases. In contrast to clean systems, these order parameters have a character of distribution functions, which change their qualitative form as we go from the normal metal to the non-Fermi liquid metal, to the insulator.

IV. TYPICAL MEDIUM THEORY FOR ANDERSON LOCALIZATION

In the following, we demonstrate how an appropriate local order parameter can be defined and self-consistently calculated, producing a mean-field like description of Anderson localization. This formulation is *not restricted* to either low temperatures or to Fermi liquid regimes, and in addition can be straightforwardly combined with well-known dynamical mean-field theories (DMFT) [36, 38, 39, 74–76] of strong correlation. In this way, our approach which we call the *Typical Medium Theory* (TMT), opens an avenue for addressing questions difficult to tackle by any alternative formulation, but which are of crucial importance for many physical systems of current interest.

Our starting point is motivated by the original formulation of Anderson [32], which adopts a *local* point of view, and investigates the possibility for an electron to *delocalize* from a given site at large disorder. This is most easily accomplished by concentrating on the (unaveraged) local density of electronic states (LDOS)

$$\rho_i(\omega) = \sum_n \delta(\omega - \omega_n) |\psi_n(i)|^2. \quad (1)$$

In contrast to the global (averaged) density of states (ADOS) which is not critical at the Anderson transition, the LDOS undergoes a qualitative change upon localization, as first noted by Anderson [32]. This follows from the fact that LDOS directly measures the local amplitude of the electronic wavefunction. As the electrons localize, the local spectrum turns from a continuous to an essentially discrete one [32], but the *typical* value of the LDOS vanishes. Just on the metallic side, but very close to the transition, these delta-function peaks turn into long-lived resonance states and thus acquire a finite *escape rate* from a given site. According to Fermi's golden rule, this escape rate can be estimated [32] as $\tau_{esc}^{-1} \sim t^2 \rho$, where t is the inter-site hopping element, and ρ is the density of local states of the immediate neighborhood of a given site.

The *typical* escape rate is thus determined by the typical local density of states (TDOS), so that the TDOS directly determines the conductivity of the electrons. This simple argument strongly suggests that the TDOS should be recognized as an appropriate order parameter at the Anderson transition. Because the relevant distribution function for the LDOS becomes increasingly broad as the transition is approached, the desired typical value is well represented by the *geometric average* $\rho_{\text{TYP}} = \exp\{\langle \ln \rho \rangle\}$. Interestingly, recent scaling analyses [77, 78] of the multi-fractal behavior of electronic wavefunctions near the Anderson transition has independently arrived at the same conclusion, identifying the TDOS as defined by the geometric average as the fundamental order parameter.

A. Self-consistency conditions

To formulate a self-consistent theory for our order parameter, we follow the “cavity method,” a general strategy that we borrow from the DMFT [36]. In this approach, a given site is viewed as being embedded in an effective medium characterized by a local self energy function $\Sigma(\omega)$. For simplicity, we concentrate on a single band tight binding model of noninteracting electrons with random site energies ε_i with a given distribution $P(\varepsilon_i)$. The corresponding local Green's function then takes the form

$$G(\omega, \varepsilon_i) = [\omega - \varepsilon_i - \Delta(\omega)]^{-1}. \quad (2)$$

Here, the “cavity function” is given by

$$\Delta(\omega) = \Delta_o(\omega - \Sigma(\omega)) \equiv \Delta' + i\Delta'', \quad (3)$$

and

$$\Delta_o(\omega) = \omega - 1/G_o(\omega), \quad (4)$$

where the lattice Green's function

$$G_o(\omega) = \int_{-\infty}^{+\infty} d\omega' \frac{\rho_0(\omega')}{\omega - \omega'} \quad (5)$$

is the Hilbert transform of the bare density of states $\rho_0(\omega)$ which specifies the band structure.

Given the effective medium specified by a self-energy $\Sigma(\omega)$, we are now in the position to evaluate the order parameter, which we choose to be the TDOS as given by

$$\rho_{\text{typ}}(\omega) = \exp \left\{ \int d\varepsilon_i P(\varepsilon_i) \ln \rho(\omega, \varepsilon_i) \right\}, \quad (6)$$

where the LDOS $\rho(\omega, \varepsilon_i) = -\frac{1}{\pi}\text{Im}G(\omega, \varepsilon_i)$, as given by Eqs. 2-5. To obey causality, the Green's function corresponding to $\rho_{\text{typ}}(\omega)$ must be specified by analytical continuation, which is performed by the Hilbert transform

$$G_{\text{typ}}(\omega) = \int_{-\infty}^{+\infty} d\omega' \frac{\rho_{\text{typ}}(\omega')}{\omega - \omega'}. \quad (7)$$

Finally, we close the self-consistency loop by setting the Green's functions of the effective medium be equal to that corresponding to the local order parameter, so that

$$G_{\text{em}}(\omega) = G_o(\omega - \Sigma(\omega)) = G_{\text{typ}}(\omega). \quad (8)$$

It is important to emphasize that our procedure defined by Eqs. 2-8 is not specific to the problem at hand. The same strategy can be used in any theory characterized by a local self-energy. The only requirement specific to our problem is the definition of the TDOS as a local order parameter given by Eq.6. If we choose the *algebraic* instead of the geometric average of the LDOS, our theory would reduce to the well-known coherent potential approximation (CPA) [79], which produces excellent results for the ADOS for any value of disorder, but finds no Anderson transition. Thus TMT is a theory having a character very similar to CPA, with a small but crucial difference - the choice of the correct order parameter for Anderson localization.

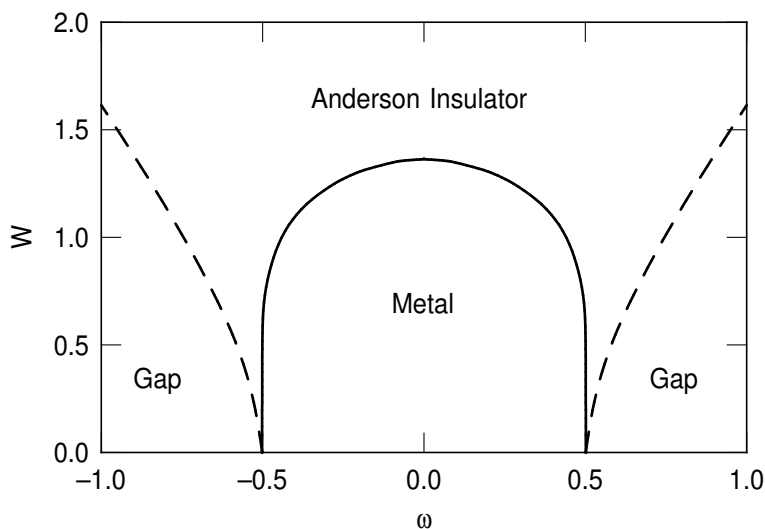


Figure 8: Phase diagram for the “semicircular” model. The trajectories of the mobility edge (full line) and the CPA band edge (dashed line) are shown as a function the disorder strength W .

In our formulation, as in DMFT, all the information about the electronic band structure is contained in the choice of the bare DOS $\rho_0(\omega)$. It is not difficult to solve Eqs. 2-8 numerically, which can be efficiently done using Fast Fourier transform methods [36]. We have done so for several model of bare densities of states, and find that most of our qualitative conclusions do not depend on the specific choice of band structure. We illustrate these findings using a simple “semicircular” model for the bare DOS given by $\rho_0(\omega) = \frac{4}{\pi}\sqrt{1 - (2\omega)^2}$, for which $\Delta_o(\omega) = G_o(\omega)/16$ [36]. Here and in the rest of this paper all the energies are expressed in units of the bandwidth, and the random site energies ε_i are uniformly distributed over the interval $[-W/2, W/2]$. The evolution of the TDOS as a function of W is shown in Fig. 10. The TDOS is found to decrease and eventually vanish even at the band center at $W \approx 1.36$. For $W < W_c$, the part of the spectrum where TDOS remains finite corresponds to the region of extended states (mobile electrons), and is found to shrink with disorder, indicating that the band tails begin to localize. The resulting phase diagram is presented in Fig. 8, showing the trajectories of the mobility edge (as given by the frequency where the TDOS vanishes for a given W , and the band edge where the ADOS as calculated by CPA vanishes).

B. Critical behavior

Further insight in the critical behavior is obtained by noting that near $W = W_c$ it proves possible to analytically solve Eqs. 2-8. Here we discuss the the critical exponent of the Anderson metal-insulator transition within the TMT model. We will demonstrate that the critical exponent β with which the order parameter Δ'' vanishes at the transition is, in contradiction to the general expectations [71], non-universal in this model.

1. *Critical behavior in the middle of the band $\omega = 0$*

To start with, let us concentrate at the band center ($\omega = 0$), and expand Eqs. 2-8 in powers of the order parameter Δ'' . In the limit of $\omega = 0$ self-consistency equations quantities Δ , \overline{G} , and Σ become purely imaginary, and near the critical disorder typical Green's function can be expanded in powers of the parameter Δ'' :

$$\begin{aligned} \overline{G(\omega, \varepsilon_i)} &= i\Delta'' = \left\langle \frac{\Delta''}{(\omega - \varepsilon_i - \Delta')^2 + \Delta''^2} \right\rangle_{\text{typ}} \\ &= i\Delta'' \exp \left[- \int d\varepsilon P(\varepsilon_i) \log[\varepsilon_i^2 + \Delta''^2] \right] = i\Delta'' f(\Delta'') \approx i\Delta''(a - b\Delta'') \end{aligned} \quad (9)$$

where

$$a = f(0) = \exp \left[-2 \int d\varepsilon P(\varepsilon) \log |\varepsilon| \right] \quad (10)$$

$$\begin{aligned} b &= \left. \frac{\partial f}{\partial \Delta} \right|_{\Delta=0} = a \cdot \exp \left[-2 \int d\varepsilon P(\varepsilon) \frac{-2\Delta''}{\varepsilon^2 + \Delta''^2} \right] \\ &= -a \int d\varepsilon P(\varepsilon) 2\pi\delta(\varepsilon) = -2\pi a P(0), \end{aligned} \quad (11)$$

and after trivial algebraic operations our self-consistency equations 2-8 reduce to a single equation for the order parameter Δ''

$$\Delta'' = \frac{\Delta''}{t^2} (a - b\Delta'') \int_{-2t}^{2t} \rho_0(\varepsilon) \varepsilon^2 d\varepsilon. \quad (12)$$

Equation 12 shows that near the transition along $\omega = 0$ direction our order parameter Δ'' vanishes linearly (critical exponent $\beta = 1$) independently of the choice of bare lattice DOS ρ_0 . In specific case of semicircular bare DOS, where

$$\Delta'' = a\Delta'' - b\Delta''^2. \quad (13)$$

the transition where Δ'' vanishes is found at $a = 1$, giving $W = W_c = e/2 = 1.3591$, consistent with our numerical solution. Near the transition, to leading order

$$\rho_{typ}(W) = -\frac{\Delta''}{\pi} = \left(\frac{4}{\pi} \right)^2 (W_c - W), \quad (14)$$

2. *Critical behavior near the band edge $\omega = \omega_c$*

In order to analytically examine scaling the critical behavior at finite ω , for simplicity we focus on a semi-circular bare DOS, where self-consistency Eqs 2-8 are greatly simplified

$$\overline{G(\omega, \varepsilon_i)} = \Delta' + i\Delta'' \Rightarrow \Delta'' = -\pi\rho_{typ} = \text{Im}\overline{G(\omega, \varepsilon_i)} \quad (15)$$

$$\Delta''(\omega) = -\exp \left\{ \int d\varepsilon_i P(\varepsilon_i) \ln \left[\frac{-\Delta''}{(\omega - \varepsilon_i - \Delta')^2 + \Delta''^2} \right] \right\} \quad (16)$$

$$\Delta'(\omega) = -H[\Delta''(\omega)], \quad (17)$$

however as in previous section, we expect the critical exponent to be the same for *any* bare DOS.

To find the general critical behavior near the mobility edge, we need to expand Eq. 16 in powers of Δ''

$$\Delta'' = \Delta'' \exp \left\{ - \int d\varepsilon_i P(\varepsilon_i) \ln [(\omega - \varepsilon_i - \Delta')^2 + \Delta''^2] \right\} \equiv \Delta'' f(\Delta''), \quad (18)$$

which cannot be done explicitly, since Δ' and Δ'' are related via Hilbert transform, which depends on the entire function $\Delta''(\omega)$, and not only on its form near $\omega = \omega_c$. Nevertheless the quantity $\omega - \Delta'(\omega)$ assumes a well-defined

W -dependent value at the mobility edge $\omega_c = \omega_c(W)$, making it possible for us to determine a *range* of values a critical exponent β may take.

After expanding $f(\Delta'') = 1$ defined by Eq. 18

$$\begin{aligned}
f(\Delta'') &= a - b\Delta'' + O(\Delta''^2) \\
a &= f(0) = \exp \left\{ -2 \int d\varepsilon P(\varepsilon) \ln |\omega - \varepsilon - \Delta'(\omega)| \right\} \\
b &= \left. \frac{\partial f}{\partial \Delta''} \right|_{\Delta''=0} = a \lim_{\Delta'' \rightarrow 0} \left[\int d\varepsilon P(\varepsilon) \frac{2\Delta''}{(\omega - \varepsilon - \Delta')^2 + \Delta''^2} \right] \\
&= a \int d\varepsilon P(\varepsilon) 2\pi \delta(\omega - \varepsilon - \Delta') = 2\pi a P(\omega - \Delta'),
\end{aligned} \tag{19}$$

we find that to the leading order Δ'' has the following ω dependence ($\delta a \equiv 1 - a$)

$$\begin{aligned}
\Delta'' &= \frac{1}{2\pi P(\omega - \Delta')} \left[\frac{1}{a} - 1 \right] \\
&\approx \frac{1}{2\pi P(\omega_c - \Delta'(\omega_c))} \delta a(\omega) \propto \delta \omega^\beta.
\end{aligned} \tag{20}$$

The functional form of $\delta a(\omega)$ is readily found

$$a = \exp \left\{ -2 \int d\varepsilon P(\varepsilon) \ln |\omega - \varepsilon - \Delta'(\omega)| \right\} \tag{21}$$

$$\delta a(\omega) = 2 \int d\varepsilon P(\varepsilon) \frac{1}{\omega - \varepsilon - \Delta'(\omega)} (\delta \omega - \delta \Delta'(\omega)), \tag{22}$$

and combining Eqs. 20,22 we arrive to

$$\Delta'' = \Delta''_0 (\delta \omega - \delta \Delta') \quad \Delta''_0 = \frac{1}{\pi P(\omega_c - \Delta'(\omega_c))} \int d\varepsilon \frac{P(\varepsilon)}{\omega_c - \varepsilon - \Delta'(\omega_c)}. \tag{23}$$

Note that $\delta \omega$ is negative, since in the range of interest $\omega < \omega_c$. In Eq 23 $\int d\varepsilon \frac{P(\varepsilon)}{\omega_c - \varepsilon - \Delta'(\omega_c)}$ is the Hilbert transform of $P(\varepsilon)$, which is positive for $\omega_c - \Delta' > 0$ (right band edge), and it is negative for the left one, where $\delta \omega > 0$.

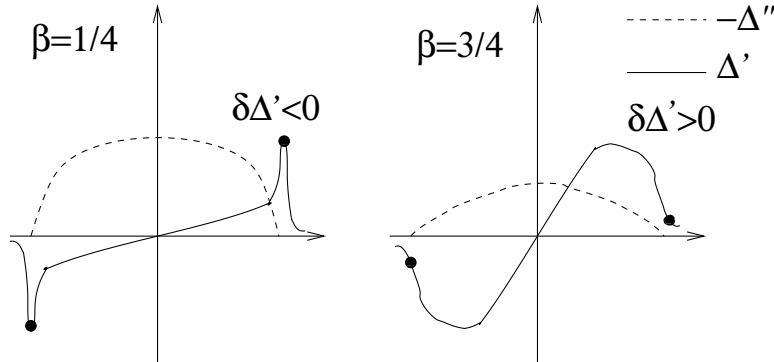


Figure 9: Requirement on $\delta \Delta'$ to be positive definite forces the value of critical exponent β to be larger than 1/2

The lower bound on critical exponent β is 0, to insure that Δ'' is convergent and vanishing at $\omega = \omega_c$. Now, if we were to assume that the leading contribution to Δ'' comes from $\delta \omega$ (and $\delta \Delta'$ can be neglected), the conclusion would be that $\Delta'' \propto \delta \omega$, and the critical exponent $\beta = 1$, just like in $\omega = 0$ case. However, this value of β is unphysical, since the Kramers-Kronig predicts Δ' to be logarithmically divergent ($\Delta' \gg \delta \omega$) when $\Delta'' \propto \delta \omega$. This is in direct contradiction with our initial statement of $\delta \omega$ being a leading contribution in Eq. 23 ($|\delta \Delta'| \ll |\delta|$), and we conclude that $\delta \Delta' \propto \delta \omega^\beta$ is the leading contribution

$$\Delta'' \approx -\Delta''_0 \delta \Delta' \propto -\delta \omega^\beta \tag{24}$$

with $\beta \in (0, 1)$. This Δ'' being a negative definite quantity imposes a constraint $\delta\Delta' > 0$, which is only satisfied for $\beta > 1/2$ (see Fig. 9, thus our critical exponent can vary in the range $\beta \in (1/2, 1)$).

Although general arguments for second-order phase transitions [71] predict universality of exponent β , we find the exponent is non-universal, which is not uncommon in some special cases of mean field theories[80]. It plausible that this critical exponent anomaly can be remedied if the MFT is extended to incorporate long range fluctuations effects beyond mean-field theory, but this remains an open problem for future work.

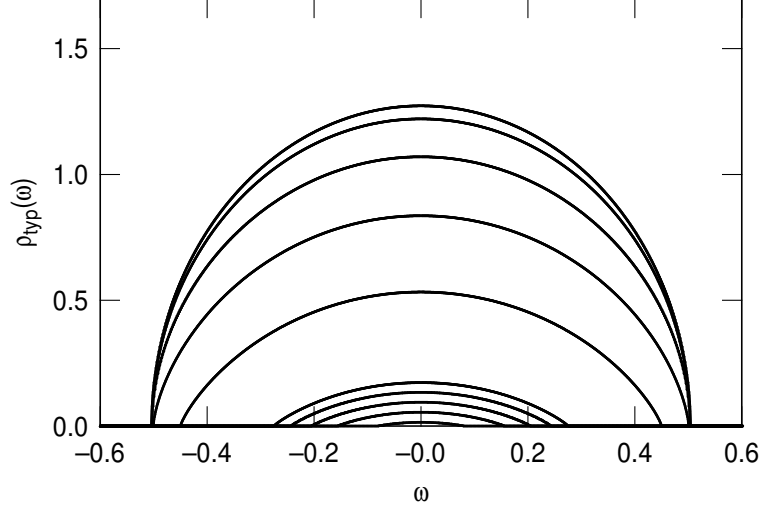


Figure 10: Typical density of states for for the SC model, for disorder values $W = 0, 0.25, 0.5, 0.75, 1, 1.25, 1.275, 1.3, 1.325, 1.35$. The entire band localizes at $W = W_c = e/2 \approx 1.359$.

3. Scaling behavior near the critical disorder $W = W_c$.

The complete analytical solution for TDOS is difficult to obtain for arbitrary ω and W . Still, the approach discussed in section IV B 1 can be extended to find a full frequency-dependent solution $\rho_{\text{typ}}(\omega, W)$ close to the critical value of disorder $W = W_c$ and which assumes a simple scaling form

$$\rho_{\text{typ}}(\omega, W) = \rho_o(W) f(\omega/\omega_o(W)). \quad (25)$$

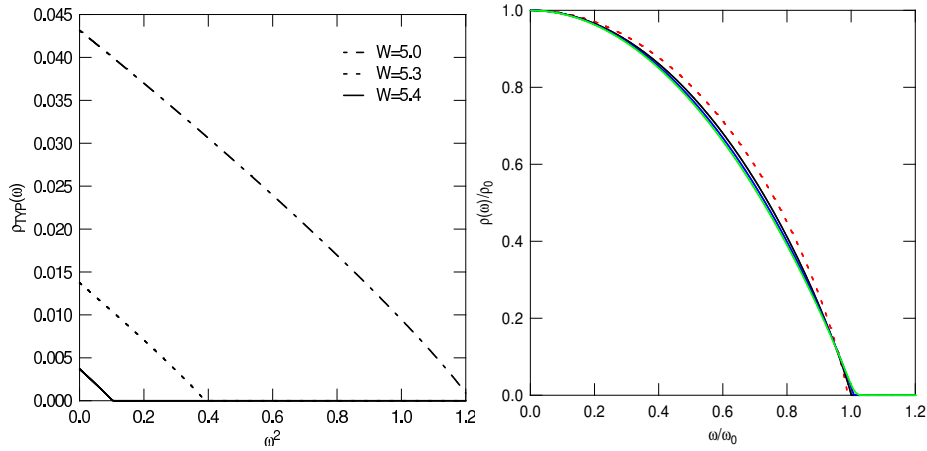


Figure 11: Left: unscaled typical DOS for various disorder displays parabolic behavior near the MIT. Right: scaling behavior near the critical disorder. The range of disorders where parabolic behavior is observed is, in fact, quite broad - $W \in (1, W_c)$, $W_c = e/2$.

Our numerical solution (see Figs. 10, 11) has suggested that the corresponding scaling function assumes a simple *parabolic* form $f(x) = 1 - x^2$

$$\rho_{\text{tyo}}(\omega) \approx \rho_0 \left(1 - \frac{\omega^2}{\omega_0^2}\right) \quad |\omega| < |\omega_0|. \quad (26)$$

In the following, we analytically calculate the scaling parameters ρ_0 and ω_0 for semicircular bared DOS and box

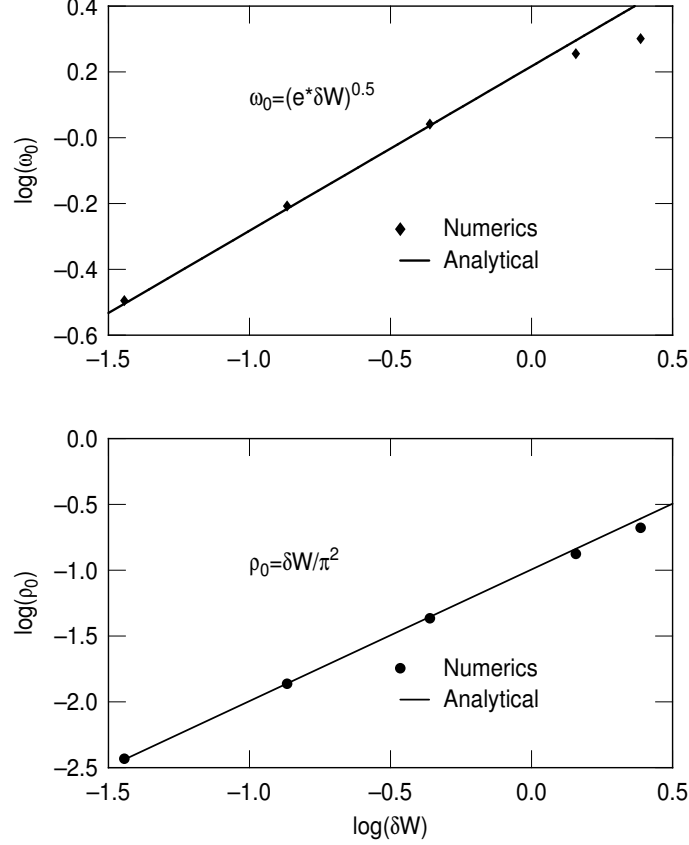


Figure 12: Scaling parameters ρ_0 and ω_0 as functions of the distance to the transition $\delta W = W_c - W$. Numerically obtained values (\diamond and \bullet) are in good agreement with analytical predictions (full line).

distribution of disorder

$$P(\varepsilon) = \begin{cases} \frac{1}{W} & \varepsilon \in \left[-\frac{W}{2}, \frac{W}{2}\right] \\ 0 & \varepsilon \notin \left[-\frac{W}{2}, \frac{W}{2}\right]. \end{cases} \quad (27)$$

$$\Delta'' = -\exp \left[\int d\varepsilon P(\varepsilon) \log \left(-\frac{\Delta''}{[(\omega - \varepsilon - \Delta')^2 + \Delta''^2]} \right) \right]$$

after averaging over disorder takes the following form

$$2W = a_- \log(\Delta''^2 + a_-^2) + a_+ \log(\Delta''^2 + a_+^2) + 2\Delta'' \left[\arctan \left(\frac{a_+}{\Delta''} \right) + \arctan \left(\frac{a_-}{\Delta''} \right) \right], \quad (28)$$

where

$$a_{\pm} = \frac{W}{2} \pm (\Delta' - \omega). \quad (29)$$

Exact expression for the real part of the cavity field Δ' is obtained by performing a Hilbert transformation of ansatz 26:

$$\begin{aligned}\Delta'' &= -\pi\rho_0 \left(1 - \frac{\omega^2}{\omega_0^2}\right) \\ \Delta' &= -H[\Delta''] = \rho_0 \left(2\frac{\omega_0\omega}{\omega_0^2} - \left(1 - \frac{\omega^2}{\omega_0^2}\right) \log \left| \frac{\omega - \omega_0}{\omega + \omega_0} \right| \right).\end{aligned}\quad (30)$$

Expanding Eqs. 28,30 to the second order in small ω results in a system of equations:

$$\begin{aligned}\frac{2\pi\rho_0}{W} \arctan\left(\frac{W}{2\pi\rho_0}\right) + \frac{1}{2} \log\left(\frac{W^2}{4} + \pi^2\rho_0^2\right) &= 1 \\ \frac{2\pi\rho_0}{W\omega_0^2} \arctan\left(\frac{W}{2\pi\rho_0}\right) &= \frac{\left(\frac{4\rho_0}{\omega_0} - 1\right)^2}{2\left(\frac{W^2}{4} + \pi^2\rho_0^2\right)},\end{aligned}$$

which can be solved for scaling parameters used the in original ansatz, Eq. 26.

$$\rho_0 = \frac{4(W_c - W)}{\pi^2} \quad (31)$$

$$\omega_0 = \sqrt{\frac{e}{2}} \sqrt{W_c - W}. \quad (32)$$

C. Numerical test of TMT

In order to gauge the quantitative accuracy of our theory, we have carried out first-principles numerical calculations for a three dimensional cubic lattice with random site energies, using exact Green functions for an open finite sample attached to two semi-infinite clean leads [41]. We computed both the average and the typical DOS at the band center as a function of disorder, for cubes of sizes $L = 4, 6, 8, 10, 12,$ and $16,$ and averages over 1000 sample realizations, in order to obtain reliable data by standard finite size scaling procedures. The TMT and CPA equations for the same model were also solved by using the appropriate bare DOS (as expressed in terms of elliptic integrals), and the results are presented in Fig. 13.

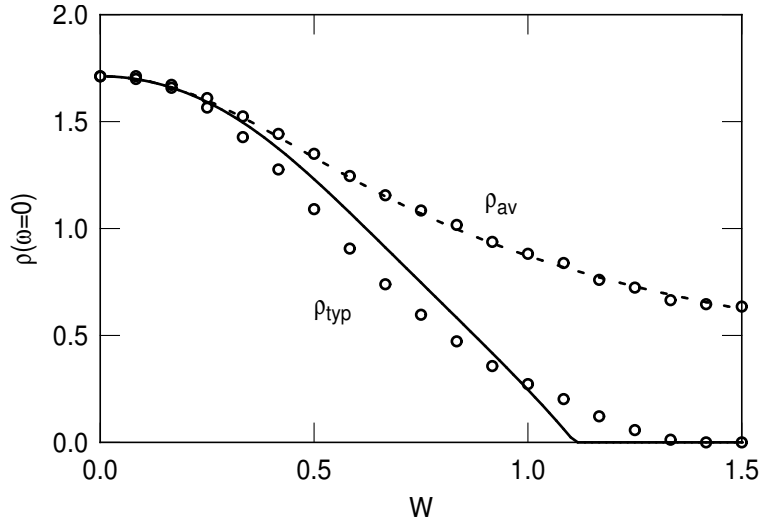


Figure 13: Typical and average DOS for a three dimensional cubic lattice at the band center ($\omega = 0$). Results from first-principle numerical calculations (circles) are compared to the predictions of TMT (for TDOS - full line) and CPA (for ADOS - dashed line).

We find remarkable agreement between these numerical data [41] and the self-consistent CPA calculations for the ADOS, but also a surprisingly good agreement between the numerical data and the TMT predictions for the TDOS order parameter. For a cubic lattice, the exact value is $W_c \approx 1.375$ [81], whereas TMT predicts a 20% smaller value $W_c \approx 1.1$. The most significant discrepancies are found in the critical region, since TMT predicts the order parameter exponent $\beta = 1$, whereas the exact value is believed to be $\beta \approx 1.5$, consistent with our numerical data. Argument based on the multi-fractal scaling analysis [77, 78], together with numerical calculations [81] of the multi-fractal spectra of wavefunction amplitudes have suggested that in three dimensions, the TDOS order parameter exponent β should be equal to the conductivity exponent $\mu \approx 1.5$. The result $\beta = \mu = 1 + O(\varepsilon)$ is also found within the $2 + \varepsilon$ approach [77, 78]. Nevertheless, we conclude that TMT is as accurate as one can expect from a simple mean-field formulation.

D. Transport properties

Most previous conventional transport theories, while providing a wonderful description of good metals, fail to describe the transport properties of highly disordered materials.

In most metals, the temperature coefficient of resistivity (TCR) α is positive, because phonon scattering decreases the electronic mean free path as the temperature is raised. The sign of TCR

$$\alpha = \frac{d \ln \rho_{res}(T)}{dT} \quad (33)$$

can be deduced from Matthiessen's rule which asserts that the total resistivity in the presence of two or more scattering mechanisms is equal to the sum of the resistivities that would result if each mechanism were the only one operating, for example:

$$\rho_{res} = \rho_{res}^{(1)} + \rho_{res}^{(2)}. \quad (34)$$

Matthiessen's rule, as stated in Eq 34 follows from the Boltzmann equation with the assumption of a wave-vector-independent relaxation time for each scattering mechanism, so if ρ_0 is the resistivity of a disordered metal at zero temperature and $\rho_{ph}(T)$ is the resistivity of the ordered material due to electron-phonon scattering, then the total resistivity at finite temperature is

$$\rho(T) = \rho_0 + \rho_{ph}(T) \geq \rho_0 \quad (35)$$

predicting that the TCR is positive ($\alpha > 0$)

Mooij [82] in 1973 have pointed out that there exist many highly disordered metals which are poor conductors and have $\rho(T) \leq \rho_0$ and negative TCRs, which clearly violate Matthiessen's rule. In fact in these materials the Boltzmann-equation formalism itself is breaking down. Apparently what is happening is that, because of the strong disorder and resulting multiple correlated scattering, the Boltzmann hypothesis of independent scattering events fails. The simple picture of temperature fluctuations impeding transport of electrons (positive TCR) is now replaced with the temperature fluctuations releasing the localized electrons and increasing the conductivity (negative TCR). When the transport properties are addressed within the TMT, the interplay of several localization mechanisms is considered, which is capable of producing the negative TCRs observed in highly disordered materials.

We start addressing the transport properties of our system within the TMT by pointing out that the escape rate from a given site can be rigorously defined in terms of the cavity field (see Eq. 2), and using our solution of the TMT equations, we find $\tau_{esc}^{-1} = -\text{Im}\Delta(0) \sim \rho_{\text{TYP}} \sim (W_c - W)$. To calculate the conductivity within our local approach, we follow a strategy introduced by Girvin and Jonson (GJ) [83], who pointed out that close to the localization transition, the conductivity can be expressed as $\sigma = \Lambda a_{12}$, where Λ is a vertex correction that represents hops to site outside of the initial pair i and j , and a_{12} is a two-site contribution to the conductivity, that can be expressed as

$$a_{12} = \langle A_{12}A_{21} - A_{11}A_{22} \rangle, \quad (36)$$

where $A_{ij} = -\text{Im}G_{ij}$ is the spectral function corresponding to the nearest neighbor two-site cluster, $\langle \dots \rangle$ represents the average over disorder.

We examine the temperature dependence of the conductivity as a function of W . Physically, the most important effect of finite temperatures is to introduce finite inelastic scattering due to interaction effects. At weak disorder, such inelastic scattering increases the resistance at higher temperatures, but in the localized phase it produces the opposite effect, since it suppresses interference processes and localization. To mimic these inelastic effects within our noninteracting calculation, we introduce by hand an additional scattering term in our self-energy, viz. $\Sigma \rightarrow \Sigma - i\eta$ or

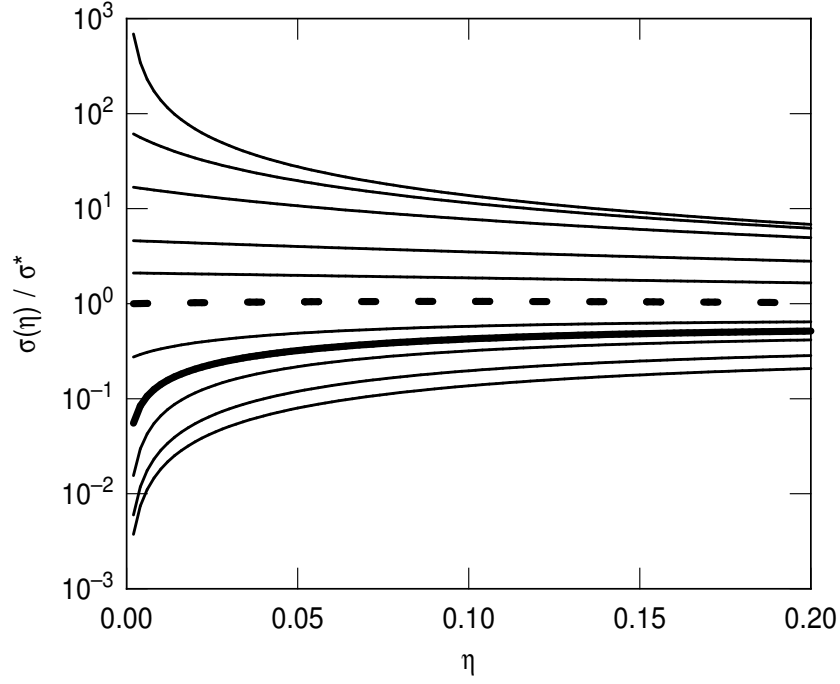


Figure 14: Conductivity as a function of the inelastic scattering rate η for for the SC model at the band center and $W = 0, 0.125, 0.25, 0.5, 0.75, 1, 1.25, \mathbf{1.36}, 1.5, 1.75, 2$. The “separatrix” ($\sigma = \sigma^*$ independent of η , i. e. temperature) is found at $W = W^* \approx 1$ (dashed line). The critical conductivity $\sigma_c(\eta) \sim \eta^{1/2}$ corresponds to $W = W_c = 1.36$ (heavy full line).

it can be treated as the imaginary part of $\omega \rightarrow \omega + \beta\eta$. The parameter η measures the inelastic scattering rate, and is generally expected to be a monotonically increasing function of temperature.

The relevant η -dependent Green’s functions G_{ij}

$$\begin{aligned} G_{ii} &= \frac{\omega + i\eta - \varepsilon_i - \Delta}{(\omega + i\eta - \varepsilon_i - \Delta)(\omega + i\eta - \varepsilon_j - t^2) - t^2} \\ G_{ij} &= \frac{t}{(\omega + i\eta - \varepsilon_i - \Delta)(\omega + i\eta - \varepsilon_j - t^2) - t^2}, \end{aligned} \quad (37)$$

reduce expression 36 to an integrable form

$$\begin{aligned} a_{12} &= 4 \frac{(\Delta'' - \eta)^2}{W^2} \times \\ &\int_{\omega - \Delta' - W/2}^{\omega - \Delta' + W/2} \frac{dx}{x^2 + (\Delta'' - \eta)^2} \arctan \left[\frac{-x + y(x^2 + (\Delta'' - \eta)^2)}{(\Delta'' - \eta)(x^2 + (\Delta'' - \eta)^2 + 1)} \right] \Bigg|_{y=\omega - \Delta' - W/2}^{y=\omega - \Delta' + W/2} \end{aligned} \quad (38)$$

that can be solved numerically as a function of temperature η and disorder W .

We have computed a_{12} by examining two sites embedded in the effective medium defined by TMT (Δ_{TMT}), thus allowing for localization effects. The vertex function Λ remains *finite* at the localization transition [84], and thus can be computed within. We have used the CPA approach to evaluate the vertex function as $\Lambda = \sigma_{\text{cpa}}/a_{12}^{\text{cpa}}$, where σ_{cpa} is the CPA conductivity calculated using approach described by Elliot [79]

$$\sigma(\omega) \propto \int_{-B/2}^{B/2} d\varepsilon \rho_0(\varepsilon) \text{Im}[G(\omega, \varepsilon)]^2 \quad (39)$$

$$\rho_0(\varepsilon) = \left(\frac{B^2}{4} - \varepsilon^2 \right)^{3/2}, \quad (40)$$

and a_{12}^{cpa} is the two-site correlation function embedded in the CPA effective medium (Δ_{CPA}). Since TMT reduces to CPA for weak disorder, our results reduce to the correct value at $W \ll W_c$, where the conductivity reduces to the

Drude-Boltzmann form. The resulting critical behavior of the $T = 0$ conductivity follows that of the order parameter, $\sigma \sim \rho_{\text{TYP}} \sim (W_c - W)$, giving the conductivity exponent μ equal to the order parameter exponent β , consistent with what is expected.

The resulting dependence of the conductivity as a function of η and W is presented in Fig. 14. As η (i. e. temperature) is reduced, we find that the conductivity curves “fan out”, as seen in many experiment close to the MIT [7, 68]. Note the emergence of a “separatrix”[7, 68] where the conductivity is temperature independent, which is found for $W \approx 1$, corresponding to $k_F \ell \sim 2$, consistent with some experiments [7]. At the MIT, $\sigma_c(\eta) \sim \rho_{\text{TYP}}(\eta) \sim \eta^{1/2}$.

V. MOTT-ANDERSON TRANSITIONS

A. Two-fluid picture of Mott

A first glimpse of the basic effect of disorder on the Mott transition at half filling was outlined already by Mott, [1] who pointed out that important differences can be seen even in the strongly localized (atomic) limit.

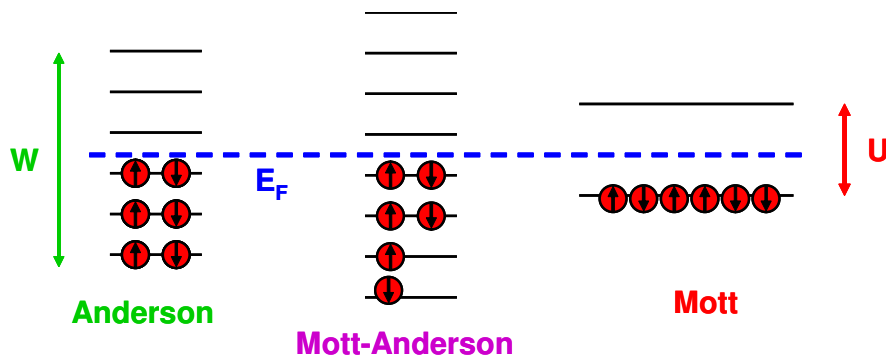


Figure 15: Energy level occupation in the strongly localized (atomic) limit. In a Mott-Anderson insulator (center), the disorder strength W is larger than the Coulomb repulsion U , and a two-fluid behavior emerges. Here, a fraction of localized states are doubly occupied or empty as in an Anderson insulator. Coexisting with those, other states remain singly occupied forming local magnetic moments, as in a Mott insulator.

For weak to moderate disorder $W < U$, the Mott insulator survives, and each localized orbital is singly occupied by an electron, forming a spin 1/2 magnetic moment. For stronger disorder ($W > U$) the situation is different. Now, a fraction of electronic states are either doubly occupied or empty, as in an Anderson insulator. The Mott gap is now closed, although a finite fraction of the electrons still remain as localized magnetic moments. Such a state can be described [39, 40] as an inhomogeneous mixture of a Mott and an Anderson insulator. A very similar “**two-fluid model**” - of coexisting local magnetic moments and conduction electrons - was proposed [85, 86] some time ago on experimental grounds, as a model for doped semiconductors. Some theoretical basis of such behavior has been discussed [37–40, 74, 87–89], but the corresponding critical behavior remains a puzzle.

This physical picture of Mott is very transparent and intuitive. But how is this strongly localized (atomic) limit approached when one crosses the metal-insulator transition from the metallic side? To address this question one needs a more detailed theory for the metal-insulator transition region, which was not available when the questions posed by Mott and Anderson were first put forward.

B. Mott or Anderson... or both?

Which of the two mechanisms dominates criticality in a given material? This is the question often asked when interpreting experiments, but a convincing answer is seldom given. To answer it precisely, one must define the appropriate criteria - order parameters - characterizing each of the two routes. The conceptually simplest theoretical framework that introduces such order parameters is given by TMT-DMFT - which we introduced in the preceding section, and discussed in detail in the noninteracting limit.. As in conventional DMFT, its self-consistent procedure formally sums-up all possible Feynman diagrams providing local contributions to the electronic self-energy [36].

When the procedure is applied to systems with both interactions and disorder systems, the self energy is still local, but may display strong-site-to-site fluctuations. Its low-energy form

$$\Sigma_i(\omega_n) = (1 - Z_i^{-1})\omega_n + v_i - \varepsilon_i + \mu,$$

defines *local* Fermi liquid parameters [39, 75]: the local quasi-particle (QP) weight Z_i , and the renormalized disorder potential v_i . This theory portrays a picture of a spatially inhomogeneous Fermi liquid, and is able to track its evolution as the critical point is approached.

In this language, Anderson localization, corresponding to the formation of bound electronic states, is identified by the emergence of discrete spectra [32] in the local density of states (LDOS). As we have seen above, this corresponds [39, 41] to the vanishing of the *typical* (geometrically averaged) LDOS $\rho_{typ} = \exp \langle \ln(\rho_i) \rangle$. In contrast, Mott localization of itinerant electrons into magnetic moments is identified by the vanishing of the local QP weights ($Z_i \rightarrow 0$). It is interesting and important to note that a very similar physical picture was proposed as the key ingredient for “**local quantum criticality**”[90], or “**deconfined quantum criticality**”[91, 92] at the $T = 0$ magnetic ordering in certain heavy fermion systems. A key feature in these theories is the possibility that Kondo screening is destroyed precisely at the quantum critical point. As a result, part of the electrons - those corresponding to tightly bound f-shells of rare earth elements - “drop out” from the Fermi surface and turn into localized magnetic moments. For this reason, it is argued, any weak-coupling approach must fail in describing the critical behavior. This is the mechanism several groups have attributed to the breakdown of the Hertz-Millis theory [93, 94] of quantum criticality, which at present is believed to be incomplete.

Precisely the same fundamental problem clearly must be addressed for the Mott-Anderson transition. The transmutation of a **fraction** of electrons into local magnetic moments again can be viewed as the suppression of Kondo screening - clearly a **non-perturbative strong correlation effect** - that should be central to understanding the critical behavior. To properly characterize it, one must keep track of the evolution of the entire distribution $P(Z_i)$ of local quasi-particle weights - which can be directly obtained from TMT-DMFT approach [41] to the Mott-Anderson transition, which we outlined above. The first applications of this new method to correlated systems with disorder was carried out in recent studies by Vollhardt and collaborators [95, 96], who numerically obtained the phase diagram for the disordered Hubbard model at half-filling, and discussed the influence of Mott-Anderson localization on magnetically ordered phases. However, the qualitative nature of the critical behavior in the Mott-Anderson transition in this model has not been examined in these studies.

C. Slave-boson solution

In the following we use complementary semi-analytical methods supplemented by Fermi-liquid theorems, in order to clarify the precise form of criticality in this model [97]. By making use of scaling properties [98, 99] of Anderson impurity models close to the MIT, we present a detailed analytic solution for this problem, which emphasizes the dependence of the system properties on its particle-hole symmetry. We consider a half-filled Hubbard model [40] with random site energies, as given by the Hamiltonian

$$H = -V \sum_{\langle ij \rangle \sigma} c_{i\sigma}^\dagger c_{j\sigma} + \sum_{i\sigma} \varepsilon_i n_{i\sigma} + U \sum_i n_{i\uparrow} n_{i\downarrow}. \quad (41)$$

Here, $c_{i\sigma}^\dagger$ ($c_{i\sigma}$) creates (destroys) a conduction electron with spin σ on site i , $n_{i\sigma} = c_{i\sigma}^\dagger c_{i\sigma}$, V is the hopping amplitude, and U is the on-site repulsion. The random on-site energies ε_i follow a distribution $P(\varepsilon)$, which is assumed to be uniform and have width W .

TMT-DMFT [41, 95] maps the lattice problem onto an ensemble of single-impurity problems, corresponding to sites with different values of the local energy ε_i , each being embedded in a typical effective medium which is self-consistently calculated. In contrast to standard DMFT [31], TMT-DMFT determines this effective medium by replacing the spectrum of the environment (“cavity”) for each site by its typical value, which is determined by the process of *geometric* averaging. For a simple semi-circular model density of states, the corresponding bath function is given by [41, 95] $\Delta(\omega) = V^2 G_{typ}(\omega)$, with $G_{typ}(\omega) = \int_{-\infty}^{\infty} d\omega' \rho_{typ}(\omega') / (\omega - \omega')$ being the Hilbert transform of the geometrically-averaged (typical) local density of states (LDOS) $\rho_{typ}(\omega) = \exp\{\int d\varepsilon P(\varepsilon) \ln \rho(\omega, \varepsilon)\}$. Given the bath function $\Delta(\omega)$, one first needs to solve the local impurity models and compute the local spectra $\rho(\omega, \varepsilon) = -\pi^{-1} \text{Im} G(\omega, \varepsilon)$, and the self-consistency loop is then closed by the the geometric averaging procedure.

To qualitatively understand the nature of the critical behavior, it is useful to concentrate on the low-energy form for the local Green’s functions, which can be specified in terms of two Fermi liquid parameters as

$$G(\omega, \varepsilon_i) = \frac{Z_i}{\omega - \tilde{\varepsilon}_i - Z_i \Delta(\omega)}, \quad (42)$$

where Z_i is the local quasi-particle (QP) weight and $\tilde{\varepsilon}_i$ is the renormalized site energy [31]. The parameters Z_i and $\tilde{\varepsilon}_i$ can be obtained using any quantum impurity solver, but to gain analytical insight here we focus on the variational calculation provided by the “four-boson” technique (SB4) of Kotliar and Ruckenstein [100], which is known to be quantitatively accurate at $T = 0$. The approach consists of determining the site-dependent parameters e_i , d_i and $\tilde{\varepsilon}_i$ by the following equations

$$-\frac{\partial Z_i}{\partial e_i} \frac{1}{\beta} \sum_{\omega_n} \Delta(\omega_n) G_i(\omega_n) = Z_i (\mu + \tilde{\varepsilon}_i - \varepsilon_i) e_i, \quad (43)$$

$$-\frac{\partial Z_i}{\partial d_i} \frac{1}{\beta} \sum_{\omega_n} \Delta(\omega_n) G_i(\omega_n) = Z_i (U - \mu - \tilde{\varepsilon}_i + \varepsilon_i) d_i, \quad (44)$$

$$\frac{1}{\beta} \sum_{\omega_n} G_i(\omega_n) = \frac{1}{2} Z_i (1 - e_i^2 + d_i^2), \quad (45)$$

where $Z_i = 2(e_i + d_i)^2 [1 - (e_i^2 + d_i^2)] / [1 - (e_i^2 - d_i^2)^2]$ in terms of e_i and d_i and $\mu = U/2$. We should stress, though, that most of our analytical results rely only on Fermi liquid theorems constraining the qualitative behavior at low energy, and thus do not suffer from possible limitations of the SB4 method.

Within this formulation, the metal is identified by nonzero QP weights Z_i on *all* sites and, in addition, a nonzero value for both the typical and the average [$\rho_{av}(\omega) = \int d\varepsilon P(\varepsilon) \rho(\omega, \varepsilon)$] LDOS. Mott localization (i.e. local moment formation) is signaled by $Z_i \rightarrow 0$ [31], while Anderson localization corresponds to $Z_i \neq 0$ and $\rho_{av} \neq 0$, but $\rho_{typ} = 0$ [32, 41]. While Ref. [95] concentrated on ρ_{typ} and ρ_{av} , we find it useful to simultaneously examine the QP weights Z_i , in order to provide a complete and precise description of the critical behavior.

D. Phase diagram

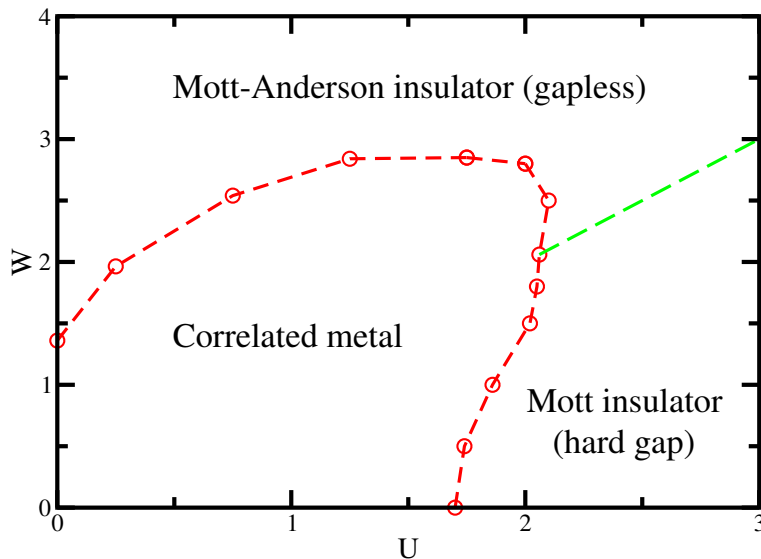


Figure 16: $T = 0$ phase diagram for the disordered half filled Hubbard model, obtained from the numerical SB4 solution of TMT-DMFT.

Using our SB4 method, the TMT-DMFT equations can be numerically solved to very high accuracy, allowing very precise characterization of the critical behavior. In presenting all numerical results we use units such that the bandwidth $B = 4V = 1$. Fig. 16 shows the resulting $T = 0$ phase diagram at half filling, which generally agrees with that of Ref. [95]. By concentrating first on the critical behavior of the QP weights Z_i , we are able to clearly and precisely distinguish the metal from the insulator. We find that at least some of the Z_i vanish all along the phase boundary. By taking a closer look, however, we can distinguish two types of critical behavior, as follows.

1. Mott-Anderson vs. Mott-like transition

For sufficiently strong disorder ($W > U$), the Mott-Anderson transition proves qualitatively different than the clean Mott transition, as seen by examining the critical behavior of the QP weights $Z_i = Z(\varepsilon_i)$. Here $Z_i \rightarrow 0$ only for $0 < |\varepsilon_i| < U/2$, indicating that only a *fraction* of the electrons turn into localized magnetic moments. The rest show $Z_i \rightarrow 1$ and undergo Anderson localization (see below). Physically, this regime corresponds to a spatially inhomogeneous system, with Mott fluid droplets interlaced with regions containing Anderson-localized quasiparticles. In contrast, for weaker disorder ($W < U$) the transition retains the conventional Mott character. In this regime $Z_i \rightarrow 0$ on all sites, corresponding to Mott localization of all electrons. We do not discuss the coexistence region found in Ref. [95], because we focus on criticality within the metallic phase. We do not find any “crossover” regime such as reported in Ref. [95] the existence of which we believe is inconsistent with the generally sharp distinction between a metal and an insulator at $T = 0$.

2. Two-fluid behavior at the Mott-Anderson transition

To get a closer look at the critical behavior of the QP weights $Z_i = Z(\varepsilon_i)$, we monitor their behavior near the transition. The behavior of these QP weights is essentially controlled by the spectral weight of our self-consistently-determined TMT bath, which we find to vanish at the transition. An appropriate parameter to measure the distance to the transition is the bandwidth t of the bath spectral function, which is shown in Fig. 17.

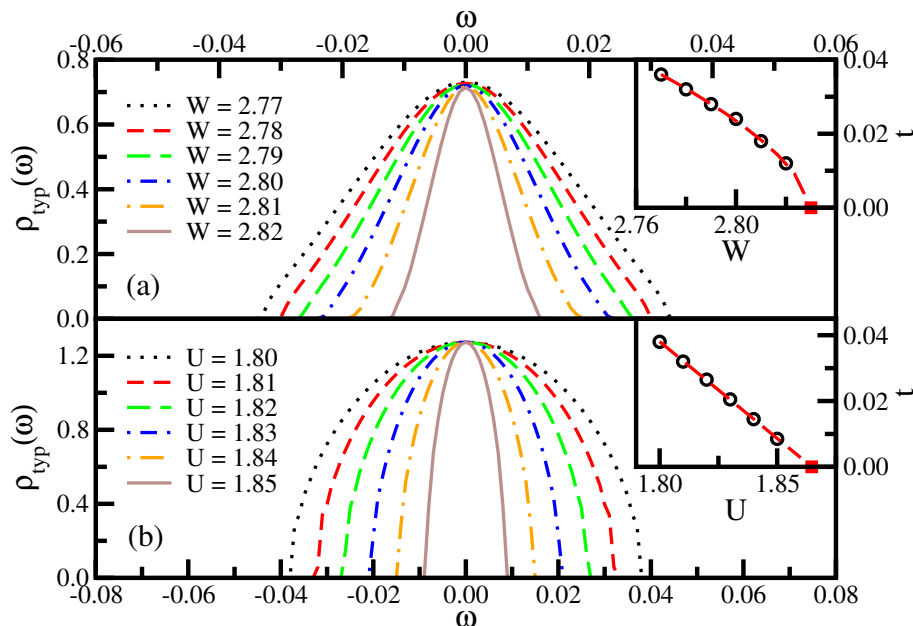


Figure 17: Frequency dependence of the typical DOS very close to the metal-insulator transition for (a) the Mott-Anderson transition ($W > U$) at $U = 1.25$ and (b) the Mott-like transition ($W < U$) at $W = 1.0$. The insets show how, in both cases, the $\rho_{typ}(\omega)$ bandwidth $t \rightarrow 0$ at the transitions.

Considering many single-impurity problems, we observe a two-fluid picture, just as in the limit earlier analyzed by Mott. [1] Indeed, these results correspond to the same atomic limit discussed by Mott, since, although the hopping itself is still finite, the cavity field “seen” by the impurities goes to zero in the current case.

As in the atomic limit, the sites with $|\varepsilon_i| < U/2$ turn into local moments and have vanishing quasiparticle weight $Z_i \rightarrow 0$. The remaining sites show $Z_i \rightarrow 1$, as they are either doubly occupied, which corresponds to those with $\varepsilon_i < -U/2$, or empty, which is the case for those sites with $\varepsilon_i > U/2$. Consequently, as the transition is approached, the curves $Z(\varepsilon_i, t)$ “diverge” and approach either $Z = 0$ or $Z = 1$. These values of Z can thus be identified as two stable fixed points for the problem in question, as we discuss below.

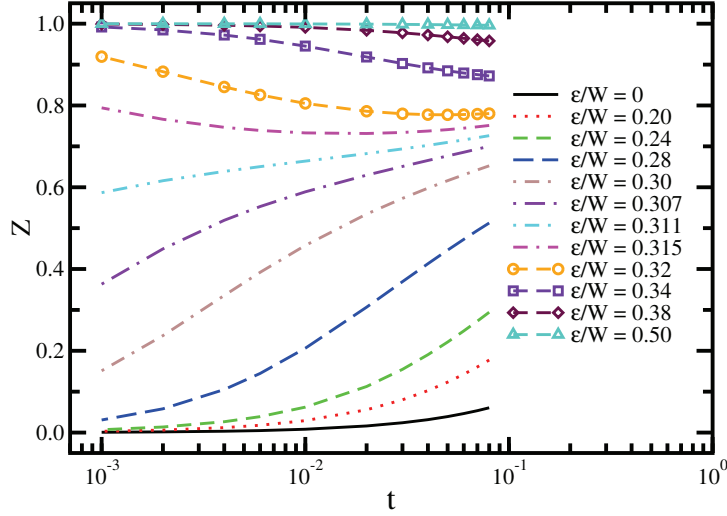


Figure 18: Quasiparticle weight Z plotted as a function of the distance to the Mott-Anderson transition t , for different values of the local site energy ϵ/W . We present the results only for positive site energies, as a similar behavior holds for negative ones.

Note that in Fig. 18 we restrict the results to positive energy values, as a similar behavior is observed for negative ϵ_i . In this case, there is precisely one value of the site energy $\epsilon_i = \epsilon^*$, for which $Z(\epsilon^*, t) \rightarrow Z^*$. This corresponds to the value of ϵ_i below which Z “flows” to 0 and above which Z “flows” to 1. In other words, it corresponds to an unstable fixed point. Just as in the atomic limit, ϵ^* is equal to $U/2$ ($\epsilon^*/W = 0.3125$ in Fig. 18, where $U = 1.75$ and $W = 2.8$).

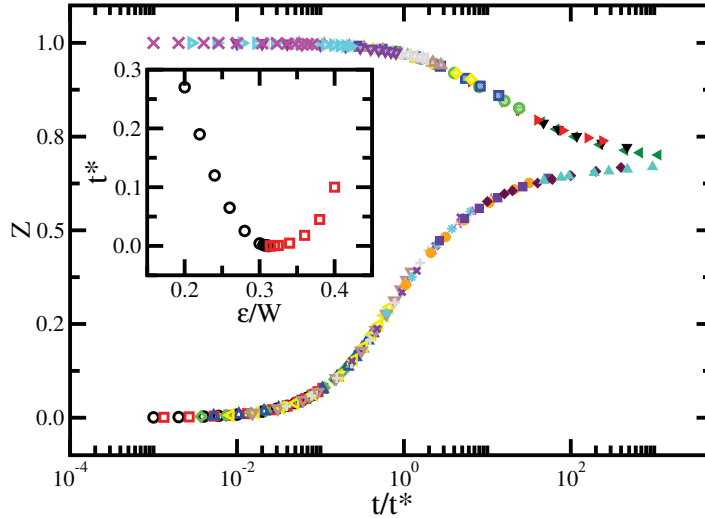


Figure 19: Quasiparticle weight Z as a function of $t/t^*(\delta\epsilon)$ showing that the results for different ϵ can be collapsed onto a single scaling function with two branches. The results for different ϵ correspond to different symbols. The inset shows the scaling parameter t^* as a function of ϵ/W for the upper (squares) and bottom (circles) branches.

3. β -function formulation of scaling

Our numerical solutions provide evidence that as a function of t the “charge” $Z(t)$ “flows” away from the unstable “fixed point” Z^* , and towards either stable “fixed points” $Z = 0$ or $Z = 1$. The structure of these flows show power-law scaling as the scale $t \rightarrow 0$; this suggests that it should be possible to collapse the entire family of curves $Z(t, \delta\varepsilon)$ onto a single universal scaling function

$$Z(t, \delta\varepsilon) = f[t/t^*(\delta\varepsilon)], \quad (46)$$

where the crossover scale $t^*(\delta\varepsilon) = C^\pm |\delta\varepsilon|^\phi$ around the unstable fixed point. Remarkably, we have been able to scale the numerical data precisely in this fashion, see Fig. 19, and extract the form of $t^*(\delta\varepsilon)$. We find that $t^*(\delta\varepsilon)$ vanishes in a power law fashion at $\delta\varepsilon = 0$, with exponent $\phi = 2$ and the amplitudes C^\pm differ by a factor close to two for $Z \gtrless Z^*$.

As shown in Fig. 19, the scaling function $f(x)$ where $x = t/t^*(\delta\varepsilon)$ presents two branches: one for $\varepsilon_i < \varepsilon^*$ and other for $\varepsilon_i > \varepsilon^*$. We found that for $x \rightarrow 0$ both branches of $f(x)$ are linear in x , while for $x \gg 1$ they merge, i.e. $f(x) \rightarrow Z^* \pm A^\pm x^{-1/2}$. As can be seen in the first two panels, in the limit $t \rightarrow 0$, the curve corresponding to $\varepsilon_i < U/2$ has $Z(t) = B^- t$, while that for $\varepsilon_i > U/2$ follows $1 - Z(t) = B^+ t$. These results are for a flat cavity field but, as mentioned earlier, we checked that the same exponents are found also for other bath functions, meaning that they are independent of the exact form of the cavity field. The power-law behavior and the respective exponents observed numerically in the three limits above have also been confirmed by solving the SB equations analytically [99] close to the transition ($t \rightarrow 0$).

In the following, we rationalize these findings by defining an appropriate β -function which describes all the fixed points and the corresponding crossover behavior. Let us assume that

$$\frac{dZ(t, \delta\varepsilon)}{d \ln t} = -\beta(Z) \quad (47)$$

is an explicit function of Z only, but not of the parameters t or $\delta\varepsilon$. The desired structure of the flows would be obtained if the β -function had three zeros: at $Z = 0$ and $Z = 1$ with negative slope (stable fixed points) and one at $Z = Z^*$ with positive slope (unstable fixed point). The general structure of these flows can thus be described in a β -function language similar to that used in the context of a renormalization group approach; we outline the procedure to obtain $\beta(Z)$ from the numerical data.

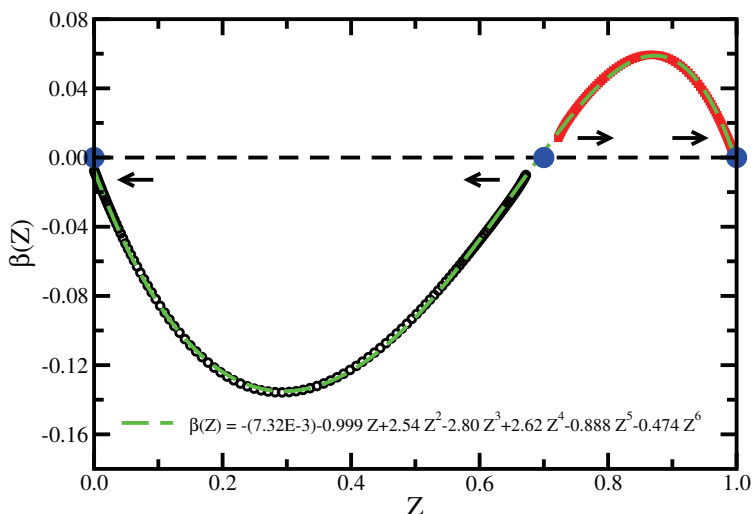


Figure 20: β -function obtained as described in the text for the Anderson impurity models close to the Mott-Anderson transition. The filled circles indicate the three fixed points found for this problem. The arrows indicate how Z flows to the stable points ($Z = 0$ and $Z = 1$) and from the unstable one ($Z \approx 0.7$).

The integration of Eq. (47) can be written in the form of Eq. (46) as

$$Z = f[t/t^*(Z_o)], \quad (48)$$

where Z_o is the initial condition (a function of $\delta\varepsilon$). With $x = t/t^*$ as before, Eq. (46) can be rewritten as

$$\beta(Z) = -x f'(x). \quad (49)$$

The numerical data for $Z = f(x)$ as a function of x is presented in Fig. 19. Thus, using Eq. (49), the β -function in terms of $x(Z)$ is determined, which can finally be rewritten in terms of Z . Carrying out this procedure, we obtain $\beta(Z)$ as shown in Fig. 20. In accordance with what was discussed above, we see that $\beta(Z)$ has three fixed points, as indicated in the figure by filled circles. $Z = 0$ and $Z = 1$ are stable, while $Z \approx 0.7$ is the unstable fixed point. The scaling behavior and the associated β -function observed here reflect the fact these impurity models have two phases (singlet and doublet) when entering the insulator. The two stable fixed points describe these two phases, while the unstable fixed point Z^* describes the phase transition, which is reached by tuning the site energy.

Interestingly, the family of curves in Fig. 18 looks similar to those seen in some other examples of quantum critical phenomena. In fact, one can say that the crossover scale t plays the role of the reduced temperature, and the reduced site energy $\delta\varepsilon = (\varepsilon_i - \varepsilon^*)/\varepsilon^*$ that of the control parameter of the quantum critical point. As the site energy is tuned at $t = 0$, the impurity model undergoes a phase transition from a singlet to a doublet ground state. Quantum fluctuations associated with the metallic host introduce a cutoff and round this phase transition, which becomes sharp only in the $t \rightarrow 0$ limit.

E. Wavefunction localization

To more precisely characterize the critical behavior we now turn our attention to the spatial fluctuations of the quasiparticle wavefunctions, we compare the behavior of the typical (ρ_{typ}) and the average (ρ_{av}) LDOS. The approach to the Mott-Anderson transition ($W > U$) is illustrated by increasing disorder W for fixed $U = 1.25$ (Fig. 21 - top panels). Only those states within a narrow energy range ($\omega < t$, see also Fig. 17) around the band center (the Fermi energy) remain spatially delocalized ($\rho_{typ} \sim \rho_{av}$), due to strong disorder screening [31, 99] within the Mott fluid (sites showing $Z_i \rightarrow 0$ at the transition). The electronic states away from the band center (i.e. in the band tails) quickly get Anderson-localized, displaying large spatial fluctuations of the wavefunction amplitudes [41] and having $\rho_{typ} \ll \rho_{av}$.

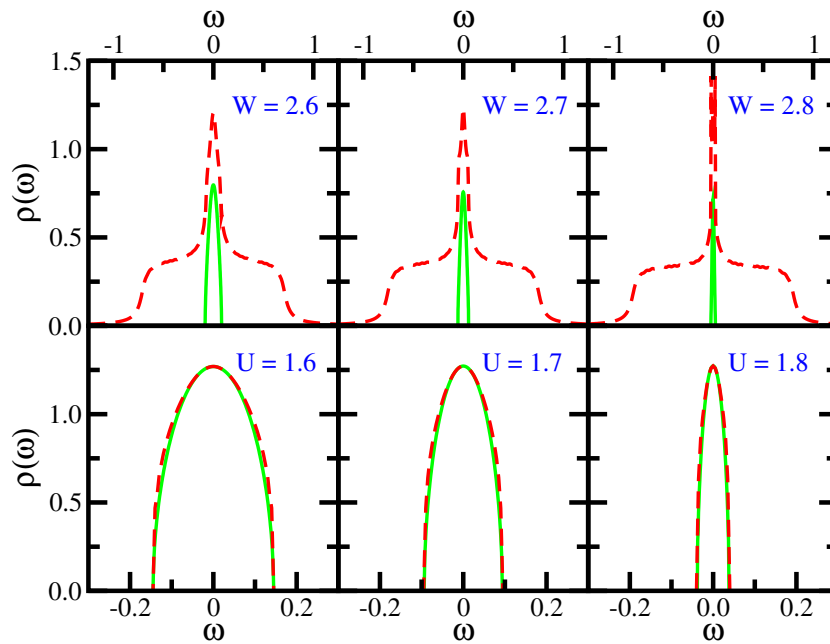


Figure 21: Frequency dependence of ρ_{typ} (full line) and ρ_{av} (dashed line) in the critical region. Results in top panels illustrate the approach to the Mott-Anderson transition ($W > U$) at $U = 1.25$; the bottom panels correspond to the Mott-like transition ($W < U$) at $W = 1.0$. For the Mott-Anderson transition, only a narrow band of delocalized states remain near the Fermi energy, corresponding to $\rho_{typ} \neq 0$. In contrast, most electronic states remain delocalized $\rho_{typ} \approx \rho_{av}$ near the Mott-like transition.

The spectral weight of the delocalized states (states in the range $\omega < t$) decreases with disorder and vanishes at the transition, indicating the Mott localization of this fraction of electrons. At this critical point, the crossover scale t also vanishes. In contrast, the *height* $\rho_{typ}(0)$ remains finite at the transition, albeit at a reduced W -dependent value, as compared to the clean limit. More precise evolution of $\rho_{typ}(0)$ is shown in Fig. 22a, demonstrating its critical jump.

Behavior at the Mott-like transition ($W < U$) is dramatically different (Fig. 21 - bottom panel). Here $\rho_{typ} \approx \rho_{av}$ over the entire QP band, indicating the absence of Anderson localization. It proves essentially identical as that established for the disordered Hubbard model within standard DMFT [31], reflecting strong correlation-enhanced screening of disorder [31, 99], where both $\rho_{av}(\omega = 0)$ and $\rho_{typ}(\omega = 0)$ approach the bare ($W = 0$) value (see also Fig. 22b). Similar results were found in Ref. [95], but an explanation was not provided.

The corresponding pinning [31, 99] for $\rho(\omega = 0, \varepsilon)$ is shown in the insets of Fig. 3, both for the Mott-Anderson and the Mott-like transition. In the Mott-Anderson case, this mechanism applies only within the Mott fluid ($|\varepsilon| < U/2$), while within the Anderson fluid ($|\varepsilon| > U/2$) it assumes smaller values, explaining the reduction of $\rho_{typ}(0)$ in this case.

F. Analytical solution

Within our SB4 approach, the TMT-DMFT order-parameter function $\rho_{typ}(\omega)$ satisfies the following self-consistency condition

$$\begin{aligned} \rho_{typ}(\omega) = \exp \int d\varepsilon P(\varepsilon) \{ & \ln[V^2 Z^2(\varepsilon) \rho_{typ}(\omega)] \\ & - \ln[(\omega - \tilde{\varepsilon}(\varepsilon) - V^2 Z(\varepsilon) \operatorname{Re} G_{typ}(\omega))^2 \\ & + (\pi V^2 Z(\varepsilon) \rho_{typ}(\omega))^2] \}. \end{aligned} \quad (50)$$

While the solution of this equation is in general difficult, it simplifies in the critical region, where the QP parameter functions $Z(\varepsilon)$ and $\tilde{\varepsilon}(\varepsilon)$ assume scaling forms which we carefully studied in previous work [99]. This simplification allows, in principle, to obtain a closed solution for all quantities. In particular, the crossover scale t , which defines the $\rho_{typ}(\omega)$ mobility edge (see Fig. 17 and Ref. [99]), is determined by setting $\rho_{typ}(\omega = t) = 0$.

Using this approach we obtain that, in the case of Mott-like transition ($W < U$), the critical behavior of all quantities reduces to that found in standard DMFT [31], including $t \sim U_c(W) - U$ (in agreement with the numerical results of Fig. 17b), perfect screening of site randomness [31, 99], and the approach of $\rho_{av}(\omega = 0)$ and $\rho_{typ}(\omega = 0)$ to the clean value. The precise form of the critical behavior for the crossover scale t is more complicated for the Mott-Anderson transition ($W > U$) (as confirmed by our numerical results in Fig. 17a), and this will not be discussed here.

Instead, we focus on elucidating the origin of the puzzling behavior of $\rho_c = \rho_{typ}(\omega = 0)$, which is known [41] to vanish linearly $\rho_c \sim (W_c - W)$ for $U = 0$, but which we numerically find to display a jump (i.e. a finite value) at criticality, as soon as interactions are turned on. For $\omega = 0$ our self-consistency condition reduces (for our model $\operatorname{Re} G_{typ}(0) = 0$ by particle-hole symmetry) to

$$\int d\varepsilon P(\varepsilon) \ln \frac{V^2 Z^2(\varepsilon)}{\tilde{\varepsilon}(\varepsilon)^2 + \pi^2 V^4 Z^2(\varepsilon) \rho_c^2} = 0, \quad (51)$$

which further simplifies as we approach the critical point. Here, the QP parameters $Z(\varepsilon) \rightarrow 0$ and $\tilde{\varepsilon}(\varepsilon) \sim Z^2(\varepsilon) \ll Z(\varepsilon)$ for the Mott fluid ($|\varepsilon| < U/2$), while $Z(\varepsilon) \rightarrow 1$ and $|\tilde{\varepsilon}(\varepsilon)| \rightarrow |\varepsilon - U/2|$ for the Anderson fluid ($|\varepsilon| > U/2$), and we can write

$$\begin{aligned} 0 = \int_0^{U/2} d\varepsilon P(\varepsilon) \ln \frac{1}{(\pi V \rho_c)^2} \\ - \int_0^{(W-U)/2} d\varepsilon P(\varepsilon) \ln [(\varepsilon/V)^2 + (\pi V \rho_c)^2]. \end{aligned} \quad (52)$$

This expression becomes even simpler in the $U \ll W$ limit, giving

$$\frac{U}{W} \ln \frac{1}{\pi V \rho_c} + a - b V \rho_c + O[\rho_c^2] = 0, \quad (53)$$

where $a(W, U) = (1 - U/W)\{1 - \ln[(W - U)/2V]\}$ and $b = \frac{2\pi^2 V}{W}$. This result reproduces the known result [41] $\rho_c \sim (W_c - W)$ at $U = 0$, but dramatically different behavior is found as soon as $U > 0$. Here, a *non-analytic*

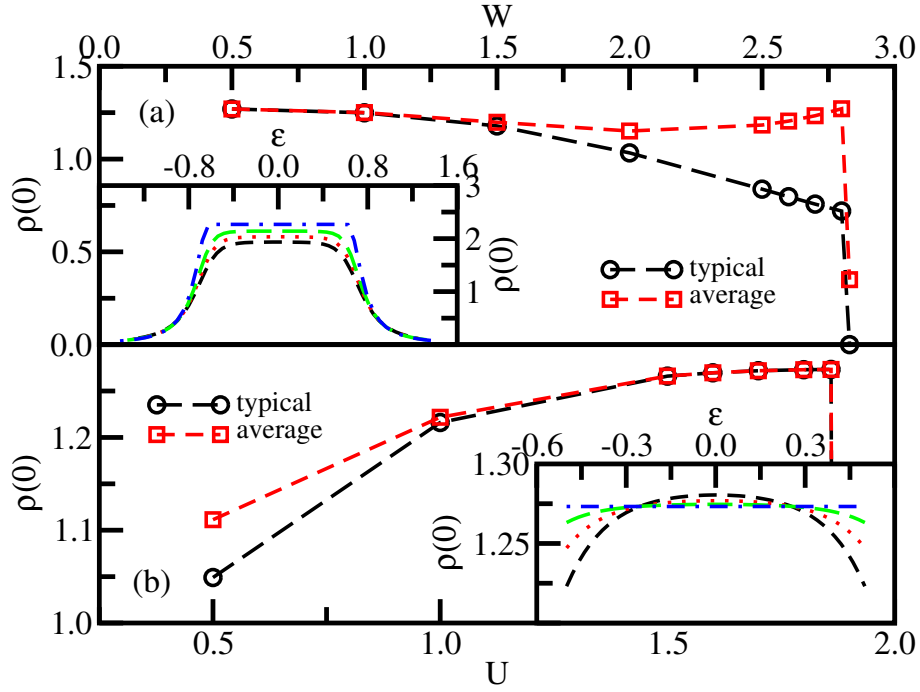


Figure 22: Typical and average values of $\rho(0)$ as the metal-insulator transition is approached for (a) $U = 1.25$ and (b) $W = 1.0$. The insets show $\rho(0)$ as a function of ϵ for (a) $W = 2.5, 2.6, 2.7$ and 2.83 (from the black curve to the blue one) and (b) $U = 1.5, 1.6, 1.7$ and 1.86 .

(singular) contribution emerges from the Mott fluid ($|\epsilon| < U/2$), which assures that ρ_c must remain finite at the critical point, consistent with our numerical results (see Fig. 22). Note that the second term in Eq. (52), coming from the Anderson fluid ($|\epsilon| > U/2$), vanishes in the case of a Mott-like transition ($U > W$), and our result reproduces the standard condition $\pi\rho_c V = 1$ [31], which corresponds to the clean limit.

A further glimpse on how the condition $\pi\rho_c V = 1$ is gradually violated as we cross on the Mott-Anderson side is provided by solving Eq. (52) for $U \gtrsim W$ limit, giving

$$\rho_c \approx \frac{1}{\pi V} \left[1 - \frac{1}{24} \left(\frac{W}{V} \right)^2 \left(1 - \frac{U}{W} \right)^3 \right], \quad (54)$$

again consistent with our numerical solution.

But what is the physical origin of the jump in ρ_c ? To see it, note that the singular form of the first term in Eq. (52) comes from the Kondo pinning[31] $\tilde{\epsilon}(\epsilon) \sim Z^2(\epsilon) \ll Z(\epsilon)$ within the Mott fluid. This behavior reflects the particle-hole symmetry of our (geometrically averaged) $\rho_{typ}(\omega = 0)$ bath function, which neglects site-to-site cavity fluctuations present, for example, in more accurate statDMFT theories [29, 30, 39, 60, 75, 76]. Indeed, in absence of particle-hole symmetry, one expects [31] $\tilde{\epsilon}(\epsilon) \sim Z(\epsilon)$, and the resulting ϵ -dependence should cut-off the log singularity responsible for the jump in ρ_c . This observation provides a direct path to further refine the TMT-DMFT approach, reconciling the present results with previous statDMFT findings [29, 30, 39, 60, 75, 76]. As a next step, one should apply the TMT ideas to appropriately chosen effective models [62], in order to eliminate those features reflecting the unrealistic particle-hole symmetry built in the current theory. We emphasize that the two-fluid picture is a consequence of only a fraction of the sites showing $Z \rightarrow 0$ and is not dependent on either particle-hole symmetry or the consequent jump in the DOS. This interesting research direction is just one of many possible future applications of our TMT-DMFT formalism.

VI. CONCLUSIONS AND OUTLOOK

This article described the conceptually simplest theoretical approach which is able to capture the interplay of strong correlation effects - the Mott physics - and the disorder effects associated with Anderson localization. It demonstrated that one can identify the signatures of both of these basic mechanisms for localization by introducing appropriate *local order parameters*, which are then self-consistently calculated within the proposed **Typical-Medium Theory**. We showed that key insight can be obtained by focusing on the evolution of the local quasiparticle weights Z_i as a *second order parameter* describing tendency to Mott localization, in addition to the Anderson-like TMT order parameter ρ_{typ} . Our main finding is that, for sufficiently strong disorder, the physical mechanism behind the Mott-Anderson transition is the formation of two fluids, a behavior that is surprisingly reminiscent of the phenomenology proposed for doped semiconductors [101]. Here, only a fraction of the electrons (sites) undergo Mott localization; the rest can be described as Anderson-localized quasiparticles. Physically, it describes spatially inhomogeneous situations, where the Fermi liquid quasiparticles are destroyed only in certain regions - the Mott droplets - but remain coherent elsewhere. Thus, in our picture the Mott-Anderson transition can be seen as reminiscent of the “orbitally selective” Mott localization [102, 103]. To be more precise, here we have a “site selective” Mott transition, since it emerges in a spatially resolved fashion. Understanding the details of such “site selective” Mott transitions should be viewed as an indispensable first step in solving the long-standing problem of metal-insulator transitions in disordered correlated systems.

Acknowledgements

The author thanks Elihu Abrahams, Carol Aguiar, Eric Andrade, Gabi Kotliar, Eduardo Miranda, Andrei Pastor, and Darko Tanasković for many years of exciting and fruitful collaboration. This work was supported by the NSF grant DMR-0542026.

-
- [1] N. F. Mott, *Metal-Insulator Transition*. (Taylor & Francis, London, 1990).
 - [2] Y. Kohsaka, C. Taylor, K. Fujita, A. Schmidt, C. Lupien, T. Hanaguri, M. Azuma, M. Takano, H. Eisaki, H. Takagi, S. Uchida, and J. C. Davis, An intrinsic bond-centered electronic glass with unidirectional domains in underdoped cuprates, *Science*. **315**, 1380, (2007).
 - [3] W. D. Wise, K. Chatterjee, M. C. Boyer, T. Kondo, T. Takeuchi, H. Ikuta, Z. Xu, J. Wen, G. D. Gu, Y. Wang, and E. W. Hudson. Imaging nanoscale Fermi surface variations in an inhomogeneous superconductor, (2008).
 - [4] A. N. Pasupathy, A. Pushp, K. K. Gomes, C. V. Parker, J. Wen, Z. Xu, G. Gu, S. Ono, Y. Ando, and A. Yazdani, Electronic origin of the inhomogeneous pairing interaction in the high-*t_c* superconductor $\text{Bi}_2\text{Sr}_2\text{CaCu}_2\text{O}_{8+d}$, *Science*. **320**, 196, (2008).
 - [5] E. Dagotto, Complexity in strongly correlated electronic systems, *Science*. **309**, 257, (2005).
 - [6] E. Miranda and V. Dobrosavljevic, Disorder-driven non-Fermi liquid behavior of correlated electrons, *Reports on Progress in Physics*. **68**, 2337, (2005).
 - [7] P. A. Lee and T. V. Ramakrishnan, Disordered electronic systems, *Rev. Mod. Phys.* **57**(2), 287 (4, 1985).
 - [8] E. Abrahams, P. W. Anderson, D. C. Licciardello, and T. V. Ramakrishnan, Scaling theory of localization: Absence of quantum diffusion in two dimensions, *Phys. Rev. Lett.* **42**, 673–676, (1979).
 - [9] F. Wegner, The mobility edge problem: continuous symmetry and a conjecture, *Phys. Rev. B*. **35**, 783, (1979).
 - [10] L. Schaffer and F. Wegner, Disordered system with *n* orbitals per site: Lagrange formulation, hyperbolic symmetry, and goldstone modes, *Phys. Rev. B*. **38**, 113, (1980).
 - [11] N. Goldenfeld, *Lectures on Phase Transitions and the Renormalization Group*. (Addison-Wesley, New York, 1992).
 - [12] K. B. Efetov, A. I. Larkin, and D. E. Khmel'nitskii, Interaction between diffusion modes in localization theory, *Zh. Eksp. Teor. Fiz.* **79**, 1120, (1980).
 - [13] A. M. Finkel'stein, Influence of Coulomb interaction on the properties of disordered metals, *Zh. Eksp. Teor. Fiz.* **84**, 168, (1983). [Sov. Phys. JETP **57**, 97 (1983)].
 - [14] A. M. Finkel'stein, *Zh. Eksp. Teor. Fiz.* **86**, 367, (1984). [Sov. Phys. JETP **59**, 212 (1983)].
 - [15] C. Castellani, C. D. Castro, P. A. Lee, and M. Ma, Interaction-driven metal-insulator transitions in disordered fermion systems, *Phys. Rev. B*. **30**, 527, (1984).
 - [16] D. Belitz and T. R. Kirkpatrick, The Anderson-Mott transition, *Rev. Mod. Phys.* **66**(2), 261 – 380 (Apr., 1994).
 - [17] A. Punnoose and A. M. Finkel'stein, Dilute electron gas near the metal-insulator transition: Role of valleys in silicon inversion layers, *Phys. Rev. Lett.* **88**, 016802(4), (2002).
 - [18] C. Castellani, B. G. Kotliar, and P. A. Lee, Fermi-liquid theory of interacting disordered systems and the scaling theory of the metal-insulator transition, *Phys. Rev. Lett.* **56**, 1179, (1987).
 - [19] R. B. Griffiths, Correlations in Ising ferromagnets. I, *J. Math. Phys.* **8**(3), 478 (Mar., 1967).

- [20] R. B. Griffiths, Nonanalytic behavior above the critical point in a random Ising ferromagnet, *Phys. Rev. Lett.* **23**, 17–19 (1 July, 1969).
- [21] H. v. Löhneysen, A. Rosch, M. Vojta, and P. Wölfle, Fermi-liquid instabilities at magnetic quantum phase transitions, *Rev. Mod. Phys.* **79**(3), 1015 (17 Aug., 2007).
- [22] S. Sachdev, *Quantum Phase Transitions*. (Cambridge University Press, UK, 1999).
- [23] T. Vojta, Rare region effects at classical, quantum and nonequilibrium phase transitions, *J. Phys. A: Math. Gen.* **39**, R143–R205 (16 May, 2006).
- [24] D. S. Fisher, Critical behavior of random transverse-field Ising spin chains, *Phys. Rev. B.* **51**(10), 6411–6461 (1 Mar., 1995).
- [25] T. Vojta, Disorder-induced rounding of certain quantum phase transitions, *Phys. Rev. Lett.* **90**, 107202 (12 Mar., 2003).
- [26] J. A. Hoyos and T. Vojta, Theory of smeared quantum phase transitions, *Phys. Rev. Lett.* **100**(24), 240601 (17 June, 2008).
- [27] V. Dobrosavljević and E. Miranda, Absence of conventional quantum phase transitions in itinerant systems with disorder, *Phys. Rev. Lett.* **94**, 187203 (11 May, 2005).
- [28] M. J. Case and V. Dobrosavljević, Quantum critical behavior of the cluster glass phase, *Phys. Rev. Lett.* **99**(14), 147204 (3 Oct., 2007).
- [29] E. Andrade, E. Miranda, and V. Dobrosavljevic, Energy-resolved spatial inhomogeneity of disordered mott systems, *Physica B: Condensed Matter.* **404**(19), 3167 – 3171, (2009).
- [30] E. C. Andrade, E. Miranda, and V. Dobrosavljevic, Electronic Griffiths phase of the d=2 Mott transition, *Physical Review Letters.* **102**, 206403, (2009).
- [31] D. Tanasković, V. Dobrosavljević, E. Abrahams, and G. Kotliar, Disorder screening in strongly correlated systems, *Phys. Rev. Lett.* **91**, 066603, (2003).
- [32] P.W.Anderson, Absence of diffusion in certain random lattices, *Phys. Rev.* **109**, 1492–1505, (1958).
- [33] N. E. Hussey, K. Takenaka, and H. Takagi, Universality of the Mott-Ioff-Regel limit in metals, *Philosophical Magazine.* **84**, 2847, (2004).
- [34] M. M. Radonjić, D. Tanasković, V. Dobrosavljević, and K. Haule, Influence of disorder on incoherent transport near the mott transition, *Phys. Rev. B.* **81**(7), 075118 (Feb, 2010).
- [35] J. G. Analytis, A. Ardavan, S. J. Blundell, R. L. Owen, E. F. Garman, C. Jeynes, and B. J. Powell, The effect of irradiation-induced disorder on the conductivity and critical temperature of the organic superconductor κ -(BEDT-TTF)₂Cu(SCN)₂, *Phys. Rev. Lett.* **96**, 177002, (2006).
- [36] A. Georges, G. Kotliar, W. Krauth, and M. J. Rozenberg, Dynamical mean-field theory of strongly correlated fermion systems and the limit of infinite dimensions, *Rev. Mod. Phys.* **68**, 13, (1996).
- [37] V. Dobrosavljević, T. R. Kirkpatrick, and B. G. Kotliar, Kondo effect in disordered systems, *Phys. Rev. Lett.* **69**, 1113, (1992).
- [38] V. Dobrosavljević and G.Kotliar, Strong correlations and disorder in d= ∞ and beyond, *Phys. Rev. B.* **50**, 1430, (1994).
- [39] V. Dobrosavljević and G.Kotliar, Mean field theory of the Mott-Anderson transition, *Phys. Rev. Lett.* **78**, 3943, (1997).
- [40] V. Dobrosavljević and G. Kotliar, Dynamical mean-field studies of metal-insulator transitions, *Philos. Trans. R. Soc. London A.* **356**, 57, (1998).
- [41] V. Dobrosavljević, A. Pastor, and B. K. Nikolić, Typical medium theory of Anderson localization: A local order parameter approach to strong disorder effects, *Europhys. Lett.* **62**, 76–82, (2003).
- [42] M. C. O. Aguiar, E. Miranda, and V. Dobrosavljević, Localization effects and inelastic scattering in disordered heavy electrons, *Phys. Rev. B.* **68**, 125104, (2003).
- [43] M. C. O. Aguiar, E. Miranda, V. Dobrosavljević, E. Abrahams, and G. Kotliar, Temperature dependent transport of correlated disordered electrons: elastic vs. inelastic scattering, *Europhys. Lett.* **67**, 226, (2004).
- [44] E. Miranda and V. Dobrosavljević, Localization effects in disordered Kondo lattices, *Physica B.* **259-261**, 359, (1999).
- [45] P. W. Anderson, Local moments and localized states, *Rev. Mod. Phys.* **50**(2), 191, (1978).
- [46] A. A. Pastor and V. Dobrosavljević, Melting of the electron glass, *Phys. Rev. Lett.* **83**, 4642, (1999).
- [47] V. Dobrosavljević, D. Tanasković, and A. A. Pastor, Glassy behavior of electrons near metal-insulator transitions, *Phys. Rev. Lett.* **90**, 016402, (2003).
- [48] D. Dalidovich and V. Dobrosavljević, Landau theory of the Fermi-liquid to electron-glass transition, *Phys. Rev. B.* **66**, 081107, (2002).
- [49] L. Arrachea, D. Dalidovich, V. Dobrosavljević, and M. J. Rozenberg, Melting transition of an Ising glass driven by a magnetic field, *Phys. Rev. B.* **69**(6), 064419 (Feb, 2004).
- [50] S. Pankov and V. Dobrosavljević, Nonlinear screening theory of the Coulomb glass, *Phys. Rev. Lett.* **94**, 046402, (2005).
- [51] M. Muller and L. B. Ioffe, Glass transition and the Coulomb gap in electron glasses, *Phys. Rev. Lett.* **93**, 256403, (2004).
- [52] S. Sachdev and N. Read, Metallic spin glasses, *J. Phys. Condens. Matter.* **8**, 9723, (1996).
- [53] A. M. Sengupta and A. Georges, Non-Fermi-liquid behavior near a T=0 spin-glass transition, *Phys. Rev. B.* **52**, 10295, (1995).
- [54] H. Westfahl Jr, J. Schmalian, and P. G. Wolynes, Dynamical mean field theory for self-generated quantum glasses, *Phys. Rev. B.* **68**, 134203, (2003).
- [55] S. Wu, J. Schmalian, G. Kotliar, and P. G. Wolynes, Solution of local-field equations for self-generated glasses, *Phys. Rev. B.* **70**(2), 024207 (Jul, 2004).
- [56] V. Dobrosavljević, T. R. Kirkpatrick, and G. Kotliar, *Phys. Rev. Lett.* **69**, 1113, (1992).
- [57] E. Miranda, V. Dobrosavljević, and G. Kotliar, Kondo disorder: a possible route towards non-Fermi liquid behavior, *J.*

- Phys.: Condens. Matter.* **8**, 9871, (1996).
- [58] E. Miranda, V. Dobrosavljević, and G. Kotliar, Disorder-driven non-Fermi liquid behavior in Kondo alloys, *Phys. Rev. Lett.* **78**, 290, (1997).
- [59] E. Miranda, V. Dobrosavljević, and G. Kotliar, Non-Fermi liquid behavior as a consequence of Kondo disorder, *Physica B.* **230**, 569, (1997).
- [60] E. Miranda and V. Dobrosavljević, Localization-induced Griffiths phase of disordered Anderson lattices, *Phys. Rev. Lett.* **86**, 264, (2001).
- [61] E. Miranda and V. Dobrosavljević, Griffiths phase of the Kondo insulator fixed point, *J. Magn. Magn. Mat.* **226-230**, 110, (2001).
- [62] D. Tanasković, E. Miranda, and V. Dobrosavljević, Effective model of the electronic Griffiths phase, *Phys. Rev. B.* **70**, 205108, (2004).
- [63] D. Tanaskovic, V. Dobrosavljevic, and E. Miranda, Spin liquid behavior in electronic Griffiths phases, *Physical Review Letters.* **95**, 167204, (2005).
- [64] B. Shklovskii and A. Efros, *Electronic Properties of Doped Semiconductors.* (Springer-Verlag, 1984).
- [65] R. N. B. M. A. Paalanen, Transport and thermodynamic properties across the metal-insulator transition, *Physica B.* **169**, 231, (1991).
- [66] S. V. Kravchenko, W. E. Mason, G. E. Bowker, J. E. Furneaux, V. M. Pudalov, and M. D'Iorio, Scaling of an anomalous metal-insulator transition in a two-dimensional system in silicon at $b = 0$, *Phys. Rev. B.* **51**, 7038, (1995).
- [67] D. Popović, A. B. Fowler, and S. Washburn, Metal-insulator transition in two dimensions: effects of disorder and magnetic field, *Phys. Rev. Lett.* **79**, 1543, (1997).
- [68] E. Abrahams, S. V. Kravchenko, and M. P. Sarachik, Colloquium: Metallic behavior and related phenomena in two dimensions, *Rev. Mod. Phys.* **73**, 251–266, (2001).
- [69] D. Simonian, S. V. Kravchenko, and M. P. Sarachik, Reflection symmetry at a $b=0$ metal-insulator transition in two dimensions, *Phys. Rev. B.* **55**(20), R13421–R13423 (May, 1997).
- [70] V. Dobrosavljević, E. Abrahams, E. Miranda, and S. Chakravarty, Scaling theory of two-dimensional metal-insulator transitions, *Phys. Rev. Lett.* **79**, 455, (1997).
- [71] N. Goldenfeld, *Lectures on phase transitions and the renormalization group.* (Addison-Wesley, Reading, 1992).
- [72] M. Rozenberg, G. Kotliar, and H. Kajueter, Transfer of spectral weight in spectroscopies of correlated electron systems, *Phys. Rev. B.* **54**, 8542, (1996).
- [73] M. Mezard, G. Parisi, and M. A. Virasoro, *Spin Glass theory and beyond.* (World Scientific, Singapore, 1986).
- [74] V. Dobrosavljević and G. Kotliar, Hubbard models with random hopping in $d=\infty$, *Phys. Rev. Lett.* **71**, 3218, (1993).
- [75] V. Dobrosavljević and G. Kotliar, Dynamical mean-field studies of metal-insulator transitions, *Phil. Trans. R. Soc. Lond. A.* **356**, 1, (1998).
- [76] E. Miranda and V. Dobrosavljevic, Disorder-driven non-Fermi liquid behaviour of correlated electrons, *Rep. Prog. Phys.* **68**, 2337–2408 (22 Aug., 2005).
- [77] M. Janssen, Statistics and scaling in disordered mesoscopic electron systems, *Phys. Rep.* **295**, 1, (1998).
- [78] A. D. Mirlin, Statistics of energy levels and eigenfunctions in disordered systems, *Phys. Rep.* **326**, 259, (2000).
- [79] P. R. J. Elliot, J. A. Krumhansl, The theory and properties of randomly disordered crystals and related physical systems, *Rev. Mod. Phys.* **46**, 465, (1974).
- [80] H. Sompolinsky and A. Zippelius, Relaxational dynamics of the edwards-anderson model and the mean-field theory of spin-glasses, *Phys. Rev. B.* **25**, 6860, (1982).
- [81] M. H. Grussbach, Determination of the mobility edge in the anderson model of localization in three dimensions by multifractal analysis, *Phys. Rev. B.* **51**, 663, (1995).
- [82] J. Mooji, Electrical conduction in concentrated disordered transition metal alloys, *Phys. Status Solidi A Phys.* **17**, 521, (1973).
- [83] M. S. M. Girvin, Dynamical electron-phonon interaction and conductivity in strongly disordered metal alloy, *Phys. Rev. B.* **22**, 3583, (1980).
- [84] S. M. Girvin and M. Jonson, Dynamical electron-phonon interaction and conductivity in strongly disordered metal alloys, *Phys. Rev. B.* **22**(8), 3583–3597 (4, 1980).
- [85] J. D. Quirt and J. R. Marko, *Phys. Rev. Lett.* **26**, 318, (1971).
- [86] M. A. Paalanen, J. E. Graebner, R. N. Bhatt, and S. Sachdev, *Phys. Rev. Lett.* **61**, 597, (1988).
- [87] M. Milovanović, S. Sachdev, and R. N. Bhatt, Effective-field theory of local-moment formation in disordered metals, *Phys. Rev. Lett.* **63**, 82, (1989).
- [88] R. N. Bhatt and D. S. Fisher, Absence of spin diffusion in most random lattices, *Phys. Rev. Lett.* **68**, 3072, (1992).
- [89] M. Lakner, H. V. Löhnneysen, A. Langenfeld, and P. Wölfle, *Phys. Rev. B.* **50**, 17064, (1994).
- [90] Q. Si, S. Rabello, K. Ingersent, and J. L. Smith, Locally critical quantum phase transitions in strongly correlated metals, *Nature.* **413**, 804, (2001).
- [91] T. Senthil, S. Sachdev, and M. Vojta, Fractionalized Fermi liquids, *Phys. Rev. Lett.* **90**, 216403, (2003).
- [92] T. Senthil, M. Vojta, and S. Sachdev, Weak magnetism and non-Fermi liquids near heavy-fermion critical points, *Phys. Rev. B.* **69**, 035111, (2004).
- [93] J. A. Hertz, Quantum critical phenomena, *Phys. Rev. B.* **14**, 1165, (1976).
- [94] A. J. Millis, Effect of a nonzero temperature on quantum critical points in itinerant fermion systems, *Phys. Rev. B.* **48** (10), 7183, (1993).
- [95] K. Byczuk, W. Hofstetter, and D. Vollhardt, Mott-Hubbard transition versus Anderson localization in correlated electron

- systems with disorder, *Phys. Rev. Lett.* **94**, 056404, (2005).
- [96] K. Byczuk, W. Hofstetter, and D. Vollhardt, Competition between Anderson localization and antiferromagnetism in correlated lattice fermion systems with disorder, *Physical Review Letters*. **102**, 146403, (2009).
 - [97] M. C. O. Aguiar, V. Dobrosavljevic, E. Abrahams, and G. Kotliar, Critical behavior at Mott-Anderson transition: a TMT-DMFT perspective, *Physical Review Letters*. **102**, 156402, (2009).
 - [98] M. C. O. Aguiar, V. Dobrosavljevic, E. Abrahams, and G. Kotliar, Scaling behavior of an Anderson impurity close to the Mott-Anderson transition, *Physical Review B*. **73**, 115117, (2006).
 - [99] M. C. O. Aguiar, V. Dobrosavljevic, E. Abrahams, and G. Kotliar, Disorder screening near the Mott-Anderson transition, *Physica B*. **403**, 1417, (2008).
 - [100] G. Kotliar and A. E. Ruckenstein, New Functional Integral Approach to Strongly Correlated Fermi Systems: The Gutzwiller Approximation as a Saddle Point, *Phys. Rev. Lett.* **57**(11), 1362, (1986).
 - [101] M. A. Paalanen, J. E. Graebner, R. N. Bhatt, and S. Sachdev, Thermodynamic Behavior near a Metal-Insulator Transition, *Phys. Rev. Lett.* **61**, 597, (1998).
 - [102] L. De Leo, M. Civelli, and G. Kotliar, T=0 heavy fermion quantum critical point as an orbital selective Mott transition, *Physical Review Letters*. **101**, 256404, (2008).
 - [103] C. Pepin, Kondo breakdown as a selective Mott transition in the Anderson lattice, *Physical Review Letters*. **98**, 206401, (2007).